LOCALIZATION OF NATRIURETIC PEPTIDE RECEPTOR-A IN THE COCHLEA

A THESIS
SUBMITTED TO THE FACULTY OF
UNIVERSITY OF MINNESOTA
BY

SARA C. PRINCE

IN PARTIAL FULFILLMENT OF THE REQUIREMENTS
FOR THE DEGREE OF
MASTER OF SCIENCE

DR. JANET FITZAKERLEY

AUGUST 2014

Acknowledgements

First and foremost, I would like to convey my genuine gratitude to my thesis advisor, Dr. Janet Fitzakerley, for her continued support, patience, and knowledge. Thank you for understanding my failures, encouraging my discoveries, and allowing me the freedom to explore unique and exciting research avenues. I am grateful for all the opportunities working with you has afforded me and I thank you for your continued support.

I would also like to express my sincere appreciation to my co-advisor, Dr. George Trachte. Thank you for always being a constant source of information and support and for keeping me on my toes.

I'm deeply grateful to the members of my committee, Dr. Jennifer Liang and Dr. Jon Holy. Jennifer, thank you for your probing questions and your suggestions. I am grateful for your ability to push me with such cordiality. Jon, thank you for all your technical support with my immunohistochemical studies. I am deeply indebted for your incredible knowledge and donation of reagents; I sincerely believe I could not have done it without your assistance.

I would also like to acknowledge Dr. Steve Downing for his consultation with renal histology. I am sincerely appreciative for your time and support. To Andrea Wolf and Bryan Bandli, thank you for your assistance with the confocal microscopy. Also, thank you to Olga Zhdankin, Dr. Sara Zimmer, and Dr. Aubie Shaw for their assistance with qRT-PCR and primer design. I am truly grateful for your technical support and assistance.

Furthermore, I would like to thank The Whiteside Technical Lab for their financial support of the laser capture microdissection experiments. Specifically, I express my gratitude to Michael Madden for all your hard work. Thank you Mike for your tireless support and patience during all our difficulties with the laser capture procedure. I am sincerely grateful for all your help and adaptability during our difficulties.

To Dr. Lynne Bemis, thank you so much for working with me on the sequencing, gel extraction, and PCR clean up. I appreciate your genuine desire to help me, and your willingness to take time out of your busy days to help with technical aspects of the procedures. Thank you for your support and encouraging words.

Furthermore, I would like to acknowledge my lab mates, Melissa Hanson, Aaron Clarke, Shelby Ryberg, and Jill Labine. Thank you guys so much for your help, your willingness to tolerate my complaints, and your encouragement. I would also like to specifically thank the lab of Dr. Jean Regal for all their support and willingness to provide supplies in a bind. Thanks Jean, Barb, and Jenna for being great lab neighbors.

Lastly, I would like to thank you, the reader, for taking the time to explore my thesis work. It takes a great deal of perseverance to write a thesis, and a bit of insanity. I often think it would take a bit more for someone to want to read one. Thank you to you, my audience, for sticking with my story.

Abstract

Natriuretic peptides have been shown to alter fluid balance and ion levels in many tissues throughout the body including the renal and cardiovascular systems[1]. When atrial natriuretic peptide (ANP) binds to its receptor (NPR-A), a dimerization event causes the activation of cGMP, initiating an internal second messenger cascade. Infusion of ANP causes improved hearing thresholds, theoretically stimulated by the secondary messengers initiated by the ANP pathway. The specific location of a natriuretic peptide receptor, NPR-A, in the inner ear including the exact mechanisms of the pathway stimulated by ANP binding, is still largely unknown.

This study was designed to test the hypothesis that (1) NPR-A is in the cells of the cochlea critical for the regulation of endolymph and ion balance and (2) NPR-A is co-localized with the effector protein NKCC1, known for its role in the movement of potassium and other ions in the inner ear.

Immunohistochemistry was performed on cryosections of cochlea collected from mice of normal hearing. Quantitative reverse-transcriptase polymerase chain reaction was also performed on kidney and cochlea homogenates, as well as laser capture microdissected cells to determine the mRNA levels of NPR-A in specific tissues.

NPR-A was localized to six cell types in the cochlea including marginal and basal cells of the stria vascularis, root cells of the spiral ligament, interdental cells and limbal fibrocytes of the spiral limbus, and spiral ganglion neurons. NPR-A expression was found in gateways critical for K^+ influx into a cellular network or efflux from a cell into the endolymph, a high K^+ extracellular fluid unique to the cochlea. Furthermore, NPR-A was also found in type I neurons that are critical for neurotransmission, implicating a regulatory role for ANP directly in the sensory pathway.

NPR-A was intermittently co-localized with NKCC1 in the marginal and interdental cells, which are both exit points for K^+ from the recycling system into the endolymph. NKCC1 may be an effector in these cells responsible for K^+ efflux into the endolymph, but is likely only one of several, as co-localization was sporadic. In other cells where NPR-A was expressed, NKCC1 was clearly not the effector activated in the ANP pathway as no co-localization was observed.

These studies provide novel information about the location of NPR-A in the cochlea and its relationship to other proteins, indicating a regulatory role for natriuretic peptides in both neurotransmission and K^+ recycling in the mouse inner ear. Globally, determining the location of NPR-A in the cochlea identifies cellular targets for future molecular study of ANP action and the mechanisms for its regulation of hearing thresholds.

Table of Contents

List of Tables

List of Figures

List of Abbreviations

- AEP- Asparaginyl endopeptidase
- ANP- Atrial natriuretic peptide
- AQP- Aquaporin
- ATP- Adenosine triphosphate
- BCs- Basal cells of the stria vascularis
- BNP- Brain natriuretic peptide
- cAMP- Cyclic adenosine monophosphate
- cDNA- Complementary DNA
- cGMP- Cyclic guanosine monophosphate
- CNP- C-type natriuretic peptide
- DNA- Deoxyribonucleic acid
- dNTPs- DNA bases
- EDTA- Ethylenediaminetetraacetic acid
- EP- Endocochlear potential
- gDNA- Genomic DNA
- GTP- Guanosine triphosphate
- ICs- Intermediate cells of the stria vascularis
- Iyd- Iodotyrosine deiodinase
- LCM- Laser capture microdissection
- LW- Lateral wall
- MCs- Marginal cells of the stria vascularis
- MET Channel- Mechanoelectrical transducer
- NCS- Normal chicken serum
- NGS- Normal goat serum
- NPPA- Natriuretic peptide precursor A
- NPR-A- Natriuretic peptide receptor A
- PB- Phosphate buffer
- PBS- Phosphate buffered saline
- PCR- Polymerase chain reaction
- PKG- Proteinkinase G
- qRT-PCR- quantitative reverse transcriptase polymerase chain reaction
- RNA- Ribonucleic acid
- SLb- Spiral limbus
- SLg- Spiral ligament
- SM- Scala media
- SPG- Spiral ganglion
- ST- Scala tympani
- StV- Stria vascularis
- SV- Scala vestibuli

Introduction

Mechanics of Hearing

The cochlea is a sensory organ with a highly specialized composition of intensely hard bone matter surrounding a delicate morphology of membranes and cell types. These tissues work together to convert a mechanical sound stimulus into a chemical signals that eventually trigger action potentials in the auditory nerve[2]. The cochlea consists of three spiral-shaped tubes filled with fluids with specific ion concentrations. Two of these tubes, the scala tympani and the scala vestibuli, contain perilymph: a high sodium, potassium solution similar to other extracellular fluids found in the body. These two scalae act to propagate the vibrations of the stapes on the oval window to the basilar membrane, where traveling cause transduction of the signal by the hair sensory cells of the organ of Corti. The scala media, which rests between the scala vestibuli and scala tympani contains endolymph, a high potassium solution. There is a high positive electrochemical potential difference from the perilymph that encases the scala media called the endocochlear potential[3].

The specialized hair cells are highly specific in both structure and function. In the human cochlea, there are 1 row of inner hair cells and 3-5 rows of outer hair cells resting on supporting cells and a membrane known as the basilar membrane. Historically, von Békésy determined that it was the basilar membrane that vibrates in response to sound at specific locations in the cochlea for a given frequency, and that this movement causes transduction of the signal into the hair cells generating receptor potentials[4].

When the basilar membrane vibrates, specialized ion channels known as the mechanoelectrical transducer (MET) channels are mechanically opened and potassium ions enter the hair cells (Fig. 1)[5,6]. These channels are located at the tips of the stereocilia and in close proximity to the tectorial membrane (Fig. 1). Once the hair cells are depolarized by the rapid K^+ influx voltage-gated calcium channels such as $Ca_V1.3$ become activated allowing for an influx of Ca^{2+} on the basolateral surface of the hair cells[7,8]. This calcium influx leads to the release of neurotransmitters causing action potentials in the auditory nerve cells. For example, inner hair cells release glutamate from the basolateral cell surface, stimulating the afferent nerve connections from type I spiral ganglion cells[3]. This signal then travels along the auditory nerve to the brain. Alternatively, when outer hair cells undergo depolarization, prestin (a voltage-triggered protein embedded in the membrane) contracts the outer hair cell which amplifies the sound-induced vibrations of the basilar membrane[3]. This outer hair cell amplification allows for the extreme threshold sensitivity experienced by mammals.

Mechanotransduction is facilitated by the large electrochemical gradient between the endolymph and the hair cells known as the endocochlear potential (EP). The endolymph has a large positive potential, roughly 80-120mV due to the flow of potassium ions (a concentration of ~150 mM). This is in comparison to the negative potential in the surrounding cells, such as the hair cells, that have a potential of around -50 mV to -70 mV and a much lower potassium concentration[3,9]. This high potassium gradient is largely produced by Kir4.1[10], a potassium inward rectifying channel present in

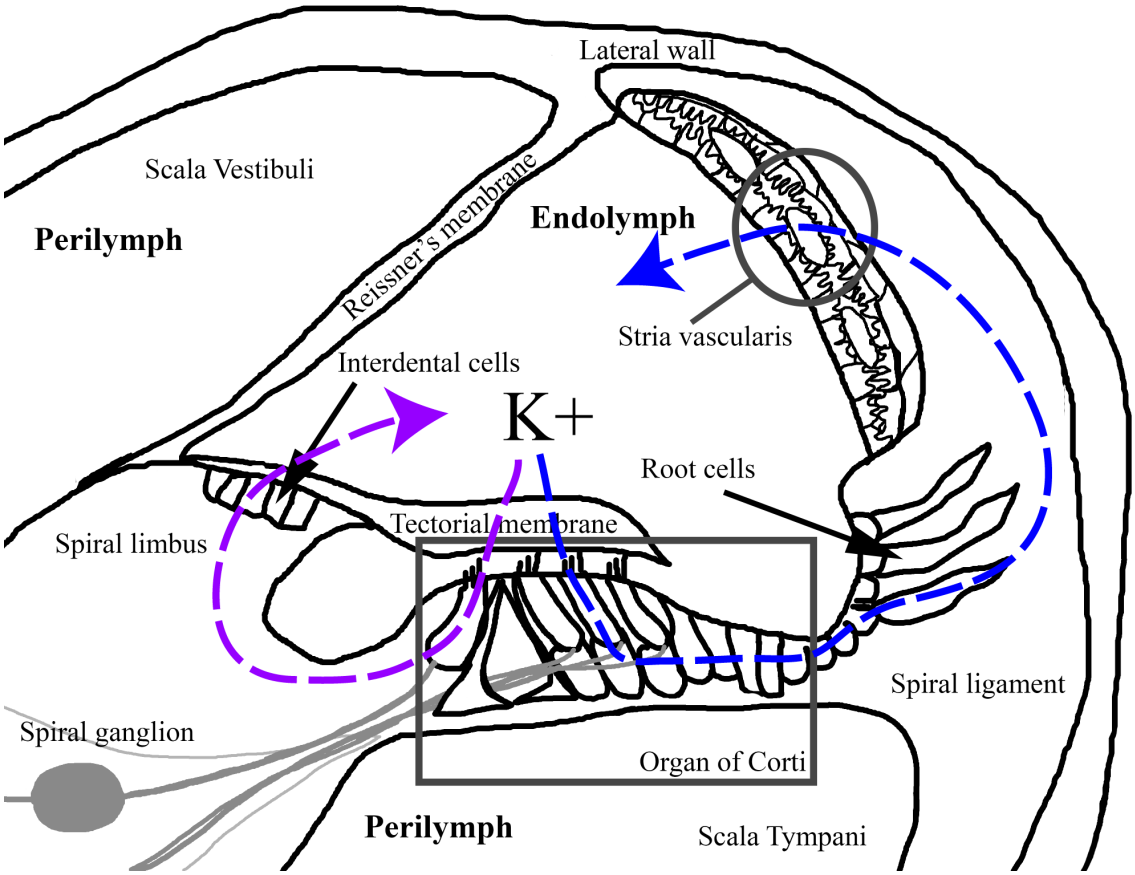

Figure 1: Anatomy and potassium recycling in the scala media.
Potassium ions flow into the inner and outer hair cells in the organ of Corti when mechanotransduction channels open. K^+ then recycles through the supporting cells/spiral ligament/stria vascularis/spiral limbus and back to the endolymph. This diagram is a cross section of the fluid filled scala media, showing portions of the scala tympani and scala vestibuli on either side. Note the stereocilia (small black lines on the apical surface of the hair cells near the tectorial membrane). The outer three hair cells are on the right, while the inner hair cell is on the left. Blue arrow depicts K^+ recycling through the outer sulcus (right) while the purple arrow represents K^+ recycling through the inner sulcus (left).

the intermediate cells of the stria vascularis (Fig. 2), a specialized epithelial tissue that maintains the ionic concentration of the endolymph.

Cochlear Anatomy

The anatomy of the cochlea has a complex morphology with specialized membranous and osseous labyrinths (Fig. 1). Within the organ of Corti alone, there are at least 12 different cell types with unique structures and functions. From an anatomical perspective, understanding the differences between regions of the cochlea is essential to understanding the functions of the different cell types. Simplistically, there are five main regions, the spiral limbus, the spiral ganglion, the organ of Corti, the spiral ligament, and the stria vascularis.

Spiral Limbus

The limbus spiralis is both boney and membranous, where the term "spiral limbus" refers only to the membranous portion of the tissue[11]. The membranous portion is derived from connective tissue and functions mainly to secrete the tectorial membrane and serve as an anchorage point for Reissner's membrane (the membrane that separates the scala media from the scala vestibuli[11]). The spiral limbus is composed of two cell types: the limbal fibrocytes necessary for ion flow and the interdental cells that secrete the tectorial membrane[11] and sequester ions from the limbal fibrocytes for export them into the endolymph[12]. One study has defined two subtypes of interdental cells and three subtypes of limbal fibrocytes[11], but for simplicity, these subtypes will not be distinguished in this thesis.

Spiral Ganglion

The spiral ganglion consists of bipolar nerve cells that have spherical cell bodies and send projections both peripherally towards the hair cells and centrally composing the auditory nerve. The cell bodies are surrounded by accessory cells known as Schwann cells that support neuronal function. There are Type I and Type II spiral ganglion neurons that vary in location and function[13]. Composing 95% of the spiral ganglion, Type I spiral ganglion neuron cell bodies are very large in size and are housed in the middle of the nerve bundle[14]. Each one sends an afferent projection that contacts only 1 inner hair cell[15]. Lateral efferent neurons from the ipsilateral lateral superior olivary complex in the cochlear nucleus coalesce on these afferent terminals for feedback[16]. Functionally, type I spiral ganglion nerves carry the action potential from the inner hair cells to the brain.

Type II spiral ganglion neurons also possess spherical cell bodies, but they are much smaller in size and are housed around the outer portions of the spiral ganglion. Type II neurons have peripheral projections that synapse on multiple outer hair cells and there are large efferent projections from the medial superior olivary complex that directly contact the outer hair cells[14]. These cells act mainly to send signals to the outer hair cells, causing the contraction event and amplification of the signal.

Organ of Corti

Named for Alfonso Giacomo Gaspare Corti, the organ of Corti is the major sensory portion of the cochlea. The organ of Corti contains many cells types with differing morphologies and functions (Fig. 1). The main function of the organ of Corti is

to convert mechanical energy from the middle ear into an electrochemical response. The organ of Corti contains specialized sensory cells known as hair cells. Hair cells are divided into two separate types, one row of inner hair cells and three to five rows of outer hair cells. The inner hair cells are more medial, and are responsible for 95% of the generation of action potentials. Conversely, outer hair cells are more lateral and act to amplify the acoustic signal[3]. Both hair cell types have afferent and efferent connections, however inner hair cells have primarily afferent connections, sending signals to the brain, and outer hair cells have mainly efferent connections receiving signals from the brain. Outer hair cells are unique in that they contain prestin in their membranes, a protein that allows for contraction of the cells upon depolarization[17]. This ability allows for further amplification of the signal.

Other than the sensory cells, the organ of Corti is mainly composed of epithelial cells that act in a supporting role. These include the inner phalangeal cells the inner hair cells rest on, the Deiter's cells that the outer hair cells rest in, and the pillar cells which support the tunnel of Corti, a space between the inner and outer cells where the type II neurons cross[3]. The supporting cells are all connected by a gap-junction network that does not cross the tunnel of Corti, creating two separate systems. The organ of Corti ends laterally with Claudius' cells and the outer sulcus cells (root cells). Medially, the organ of Corti terminates with the inner sulcus cells, that merge into the cells of the spiral limbus[11].

Spiral ligament and the gap junction network

The spiral ligament is the lateral attachment point for the basilar membrane and is embedded in the lateral wall of the cochlea (Fig. 1). Mainly composed of different fibrocyte types, the spiral ligament acts to facilitate recycling of potassium ions from the organ of Corti back to the stria vascularis[18]. In addition to fibrocytes, the spiral ligament contains root cells, sometimes called outer sulcus cells. The root cells play a major functional role in the recycling of potassium ions from the organ of Corti back to the endolymph[19]. The cell bodies of the root cells are embedded within the outer sulcus adjacent to Claudius' cells of the organ of Corti[18]. In addition to their cells bodies in the outer sulcus, the root cells extend laterally through the fibrocytes of the spiral ligament[19]. Root cells are connected to the epithelial cells of the organ of Corti via gap-junctions, but do not share these connections with the surrounding fibrocytes (an important separation in the recycling of K^+).

Stria vascularis

The stria vascularis (StV) is an epithelial tissue that lines the scala media on the lateral wall of the cochlea[20] (Fig. 1). This tissue is a major regulator of the ionic balance of endolymph that fills the scala media. The StV consists of three cell layers: most medially, the marginal cells that face the endolymph; the intermediate cells; and the basal cells that separate the stria vascularis from the spiral ligament[2,3] (Fig. 2).

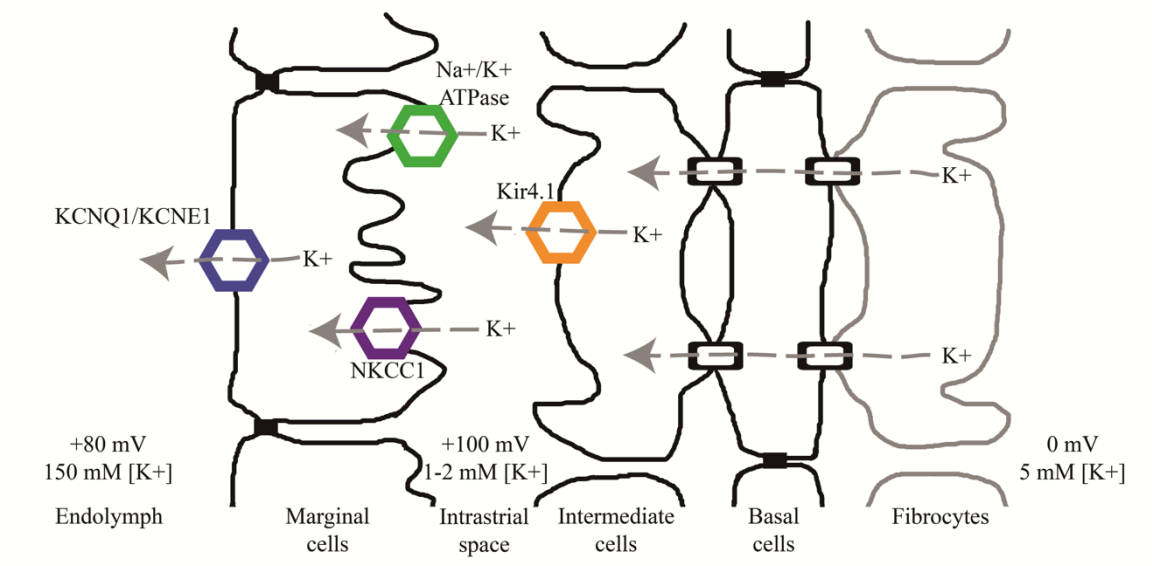

Figure 2: Structure of the stria vascularis.
Composed of three differentiated cell layers, the stria vascularis functions to maintain the endocochlear potential by recycling K^+ back into the endolymph. Gap junctions are noted as open rectangles, while tight junctions are depicted as closed black boxes. The flow of K^+ from the spiral ligament into the endolymph is represented with grey arrows and is shown moving through different transporters and channels. Note the voltage and K^+ concentrations in each cellular area.

Marginal Cells

Marginal Cells (MCs) make up the most medial portion of the stria vascularis and are directly in contact with the endolymph of the scala media. MCs are hexagonal in shape and often covered with microvilli on the endolymphatic surface, particularly in the apical turn of the cochlea [21]. The apical surface (with microvilli) is slightly round, and bulges out towards the endolymph. The basolateral surface consists of long projections that extend laterally toward the basal cells of the stria vascularis[20], creating invaginations for increased surface area and absorptive capacity[22] (Fig. 2). MCs are apically connected by tight junctions that create a barrier between the endolymph and cells of the stria vascularis[20].

One of the major functions of marginal cells is to pull K^+ from the intrastrial space and export the ions back into the endolymph. This function is performed by a variety of channels and transporters such as NKCC1, a sodium, potassium, 2-chloride symporter. NKCC1 is located on the basolateral surface of the marginal cells and acts to transport K^+ ions into the cell from the intrastrial space[23]. In mice strains engineered to lack the gene *Slc12a2* that codes for NKCC1[24], the scalae volume is decreased causing deafness. This evidence indicates that the NKCC1 co-transporter is essential for the maintenance of proper sound propagation. Once the K^+ is in the cell, it is exported out of the MCs by KCNQ1/KCNE1 channels back into the endolymph to re-establish the K^+ gradient and the EP.

Intermediate Cells

The highly specific shape of the MCs allows for the intermediate cells (ICs) to interdigitate among the MC basolateral projections. ICs are intermingled between marginal cells of the stria vascularis and are critical to establishing the endocochlear potential (EP) of the scala media (Fig. 2). ICs express the potassium inward rectifying channel Kir4.1[10]. Within the stria vascularis, Kir4.1 is only found in intermediate cells (Fig. 2), making Kir4.1 a good molecular marker for this cell type. Kir4.1 is essential to moving potassium ions out of the intermediate cells into the intrastrial space[25]. [26,27]. A 2002 study with Kir4.1 knock-out mice showed that deletion of Kir4.1 leads to a lack of endocochlear potential, reduced endolymphatic volume and potassium concentration, and diminished hearing ability[10,25].

ICs are derived from neural crest tissue and contain melanosomes, giving the cells a dark appearance [20]. One study classifies intermediate cells as basal intermediate cells and upper intermediate cells. This distinction indicates that basal intermediate cells interact with the basal cell layer of the StV, while upper intermediate cells interact only with the basolateral surface of the marginal cells[20]. While this may be an important anatomical differentiation among intermediate cell types, there are currently no functional distinctions between intermediate cells. Therefore for the sake of simplicity, this manuscript classifies intermediate cells as one cell type.

Basal Cells

The basal cells (BCs) in the stria vascularis compose a single layer of flat cells[20] adjacent to the fibrocytes in the spiral ligament[20,28]. In rats[29], cats[30], guinea pigs[22,29,31], and humans[32], BCs have projections that extend medially towards the marginal cell layer. BCs are highly permeable to K^+ and connected together by tight junctions composed of Claudin-11 to form a strong barrier at the base of the stria vascularis against the fibrocytes[2,3]. The basal barrier acts to contain the large electrical potential of the intrastrial space[9,26,33]. When Claudin-11 is knocked out, potassium concentration in the endolymph is not affected, but EP is drastically reduced from a normal level of ~80 mV to ~30 mV[34]. Theoretically, this would be because the transporters/channels that maintain the EP are still viable, but the K^+ is not sequestered in the stria vascularis, and leaks back into the underlying fibrocytes. This implicates the important role the basal cells must play in compartmentalization and maintenance of the endocochlear potential [i.e. the barrier prevents K^+ reflux back into the fibrocytes in the connective tissue gap-

junction network]. This ensures the passive influx of potassium ions into the intrastrial space cannot dissipate once basally generated[3].

Potassium flow in the cochlea

As previously mentioned, the movement of potassium in the cochlea is critical to maintaining function, and is known as the potassium recycling system. Once K^+ enters the hair cells, it has to be removed in order for the cell to repolarize. KCNQ4 (Kv7.4) is a K^+ channel embedded in the basal pole of outer hair cells that removes K^+ from outer hair cells[3]. One of the major causes of human deafness (DFNA2) is a defect in this pore, which leads to outer hair cell degeneration[35]. While the loss of the channel and its expression profile indicate Kv7.4 is critical to the movement of K^+ out of the outer hair cells, it is not the only K^+ channel integral to this process.

Once the K^+ is removed from the hair cells, it enters a gap junction network and moves laterally through the outer sulcus system up to the stria vascularis (Fig. 1, right blue arrow) or medially through the inner sulcus system and out of the spiral limbus[2,3] (Fig. 1 left purple arrow). Both of these recycling pathways are distinguished by two gap-junction networks: an epithelial gap-junction network and a connective tissue gap-junction network. Potassium movement through these systems will be discussed in the following two sections.

Potassium Recycling in the Outer Sulcus

In the outer sulcus K^+ recycling system, the epithelial gap-junction network consists of the supporting cells of the organ of Corti, while the connective tissue gap

junction network spans the spiral ligament and is mainly comprised of fibrocytes[2,19]. In the epithelial gap-junction network, K^+ ions pass through KCC3 and KCC4 transporters which shuttle K^+ ions into the Deiter's cells that underlie the outer hair cells[3,19,36]. Kir4.1 is also expressed in the Deiter's cells, supporting the influx of K^+ ions into the epithelial cells[2]. Once in the supporting cells, potassium ions flow laterally through a series of gap junctions from the Deiter's cells to the outer sulcus cells[2,37]. These gap junctions are comprised of two hemi-channels that form a pore between cells. Composed of different connexins (Cx26, Cx30, Cx32), these gap junctions passively transport molecules and ions of < 1 kDa[2].

Outer sulcus cells, often referred to as root cells, act as the transition point for K^+ ions from the epithelial gap junction system into the connective gap-junction network. These cells branch from the outer sulcus laterally into the spiral ligament between the fibrocytes[18]. There are no gap-junctions between root cells (epithelial gap junction network) and the fibrocytes of the spiral ligament (connective tissue gap junction network) meaning K^+ cannot simply move through the cells along a gradient[2,18,19]. Therefore, fibrocytes must express transporters to move K^+ ions into the connective tissue gap-junction network.

In addition to the projections from the root cells, the spiral ligament consists of 5 fibrocyte types that are differentiated by their anatomical positioning, morphologies, and the transporters and channels they express. There are many uptake proteins for K^+ and similar cations in the fibrocytes that surround the root cells. One of these is NKCC1, which acts to move 1 Na^+, 1 K^+, and 2Cl^- ions into the fibrocytes[23]. Directly abutting the

outer sulcus cell root projections (epithelial gap-junction network) are type II[18] and type IV[38] fibrocytes of the connective tissue gap-junction network. These fibrocytes are connected to other fibrocytes of the spiral ligament via gap-junctions and extend upward to connect to the basal cells of the stria vascularis. The cytoplasm in the fibrocytes is similar to perilymph, with a low K^+ concentration around 5 mM and a potential near 0 mV[4,39]. This internal environment facilitates the movement of K^+ towards the stria vascularis to encourage recycling of the ions back to the endolymph through the outer sulcus recycling system.

Potassium Recycling in the Inner Sulcus

Potassium ions can also move through the inner sulcus recycling system (Fig. 1), but the cell distribution is not as differentiated (in both the number of cell types and anatomical differences) as it is in the outer sulcus system. The functions of the cells in the inner sulcus system are much less distinct, and the physical connections between cell types are not as well defined. The inner sulcus recycling system performs roughly the same task as the outer sulcus system, with limbal fibrocytes carrying out functions synonymous with the basal strial cells as well as fibrocytes (of the spiral ligament). The observation that K^+ recycles in more than one direction is relatively new, and therefore less is known about recycling in this system.

Similar to the outer hair cells, inner hair cells move K^+ out at their basal poles. K^+ is then taken up by KCC3 in inner phalangeal cells, which do not express KCC4 like the Deiter's cells[36]. Once in the inner phalangeal cells, K^+ is in the epithelial gap-junction network along the medial inner sulcus. The transition in cell type from inner sulcus cells

to limbal fibrocytes is somewhat unclear, but at some point there is a transition in cell type from epithelial cells to limbal fibrocytes[11]. From there, interdental cells sequester cations from the underlying limbal fibrocytes, and export them out into the endolymph[12], completing the K^+ recycling system through the inner sulcus.

Natriuretic Peptides

Natriuretic peptides (NPs) and their receptors regulate sodium and potassium concentrations, blood volume, blood pressure, long bone growth, pulmonary hypertension, and ventricular hypertrophy[1]. There are three types of NPs in mammals: atrial (ANP), b-type (BNP), and c-type (CNP) natriuretic peptides. The three NPs are structurally similar, with a conserved internal ring-structure (Fig. 3). The conserved sequence begins and ends with a cysteine residue (CFGxxxDRIxxxxGLGC where X stands for any amino acid and is different for each NP), allowing formation of a disulfide bridge, giving the protein a tertiary ring-shaped structure[40] (Fig. 3). The peptide "tails" that branch off the ring structure are unique to each NP. In total, ANP has 28 amino acids and BNP has 32 amino acids. CNP has two subtypes: a 53 amino acid peptide and a 22 amino acid peptide that has a much shorter amino acid chain branching from the internal ring[1].

The three receptors for natriuretic peptides--- NPR-A, NPR-B, and NPR-C--- are located in the inner ear as well as other tissues (such as the kidney and the heart[1,41,42]). NPR-A and NPR-B are structurally similar, in that they both have an intracellular guanylyl cyclase domain, which acts to generate cGMP[43](Fig. 3). NPR-A can bind ANP and BNP, NPR-B can bind CNP, and NPR-C can bind all three peptides[1]. NPR-C does

not have an internal guanylyl cyclase domain, and unlike the other receptors, acts to degrade circulating NPs[44,45] (Fig. 3).

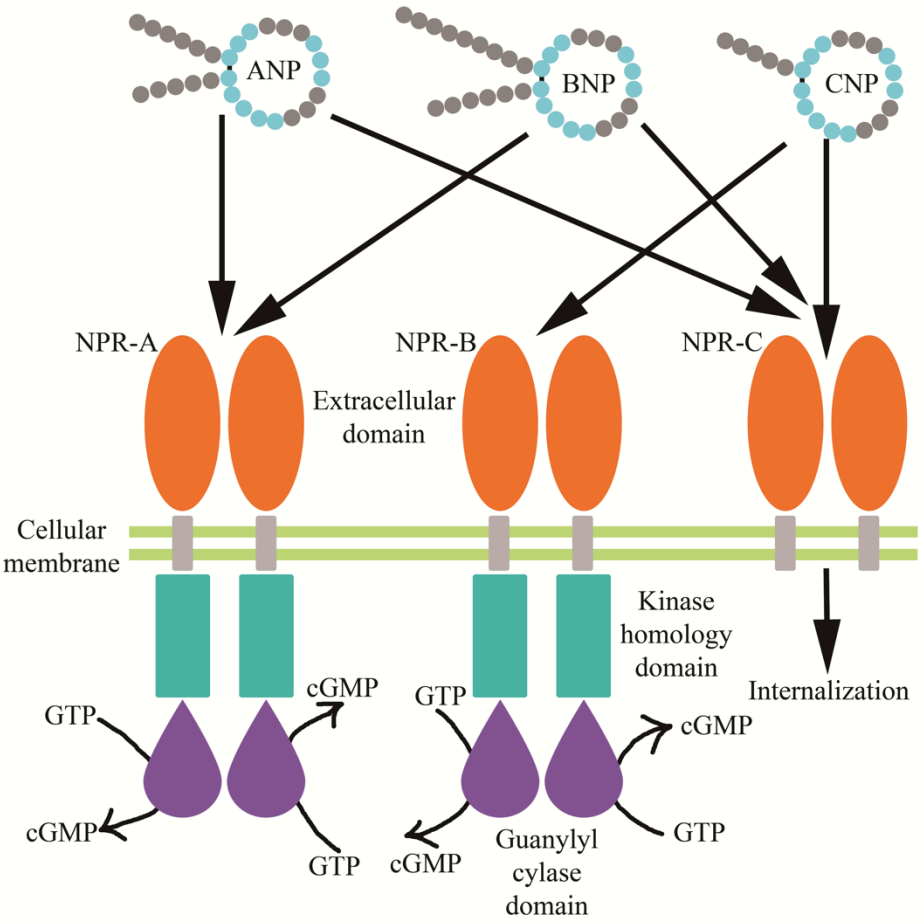

Figure 3: The three natriuretic peptides and their receptors.
The three NPs (ANP, BNP, and CNP) with the conserved internal ring structure and disulfide bridge (top) and the three natriuretic peptide receptor proteins are shown. Note the lack of internal sequence expressed by the clearance receptor NPR-C (right). NPR-A and NPR-B act to generate cGMP from GTP when an appropriate NP binds. The receptor affinity of each NP is shown by the straight black arrows. NPR-A can bind ANP and BNP, NPR-B can bind CNP, and NPR-C can bind all three peptides[1,46].

When ANP binds to its receptor, NPR-A, an external change happens to initiate a secondary messenger cascade that likely affects hearing. NPR-A and NPR-B consists of a external ligand binding domain (the active site for the appropriate NP), a membrane-spanning region, and an internal kinase homology domain that suppresses a guanylyl cyclase domain on the carboxyl terminal of the protein[44]. When ANP or BNP binds to NPR-A (Fig. 3), it causes “”molecular tightening” in response to the disulfide linkage of the incoming hormone, leading to homo-dimerization of the receptor protein[44]. This dimerization facilitates the activation of the internal kinase homology domain by ATP, which inhibits the repression of the guanylyl cyclase domain. The kinase homology domain can be phosphorylated at 4 serine and 2 threonine residues. When the kinase homology domain is activated, a conformational change occurs in the internal guanylyl cyclase domain causing the conversion of guanosine triphosphate (GTP) to cyclic guanosine monophosphate (cGMP)[46] (Fig. 3).

The availability of the second messenger compound, cGMP, leads to activation of proteinkinase G (PKG), a compound critical in many tertiary messenger systems in different cell types. PKG has many functions, but in regards to audition is hypothesized to regulate other proteins that could alter EP and lead to changes in hearing. In the kidney, one hypothesis is that ANP acts via NPR-A to activate NKCC transporters, resulting in natriuresis[1,47,48] Because of the key roles of potassium in audition, this raises the possibility that natriuretic peptides and their receptors are involved in the regulation of NKCC1 and other ion channels and transporters in the ear as well, thereby contributing to the regulation of hearing thresholds (Fig. 4).

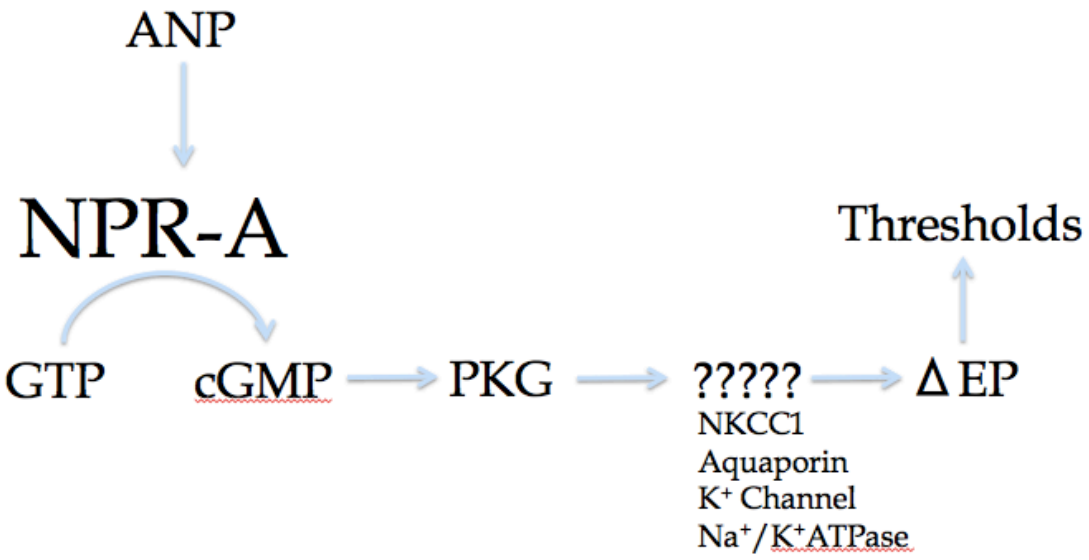

Figure 4: Hypothesized ANP pathway in the cochlea.
ANP binds to its receptor protein, in this case NPR-A. This causes a number of internal conformational changes, but ultimately jump-starts a second messenger cascade. What happens in the pathway after the generation of PKG is unclear. However, infusion information collected in our lab indicates systemic infusion of ANP causes a change in hearing thresholds, thus forming the end of the ANP pathway in the cochlea.

Previous work in our lab has shown that infusion of ANP improves hearing thresholds in mice of normal hearing. Increasing ANP by infusion in normal mice leads to both measurable improvements in hearing and increases in cochlear cGMP[49]. NPR-A knockout mice (a nonsense mutation in the gene that encodes the receptor) develop normal hearing, but experience a high frequency hearing deficit by early adulthood. Infusing ANP in these mice does not confer hearing recovery, presumably because there is no receptor for the hormone and therefore no internal changes in cGMP levels. Furthermore, cochlear cGMP levels in the NPR-A knockout mice are also decreased[50]. In other labs, NPR-A mRNA has been localized to the cochlea using in situ hybridization and RT-PCR, however, these finding do not give precise expression patterns of NPR-A in

specific cells/tissues [41,41,42,51–54]. This combination of results implies a critical regulatory role for ANP in the cochlea, and therefore we developed the following experiments to determine the location of the receptor (NPR-A) to learn which cells ANP may influence.

Hypotheses

The overarching goal of these studies is to understand the role of natriuretic peptides in the inner ear. NPs are crucial regulators of fluid balance in other tissues and therefore, may be critical in the maintenance of endolymph and endocochlear potential. This study specifically looked for the precise location of an NP receptor, NPR-A, in the cochlea to determine if its location was specific to areas critical for fluid movement. This study also examined the relationship of NPR-A to other proteins known to regulate fluid or ion movement in the cochlea such as NKCC1 and Kir4.1. Furthermore, laser capture microdissection and quantitative reverse transcriptase polymerase chain reaction were also performed to learn more about the expression of these proteins in the cochlea.

***Hypothesis 1*:** *NPR-A is located in regions of the cochlea important for the regulation of endolymph ion composition.*

Ion composition of the fluid bathing the hair cells is essential to the physiological process of hearing. If NPR-A activation results in changes to the endolymph and endocochlear potential, NPR-A should be located in regions of the cochlea that regulate fluid or ion balance. This hypothesis was broken into two components. Aim A) identified the expression pattern of NPR-A in the cochlea, while aim B) used specific

markers for different cell layers of the StV to determine more specifically where NPR-A was expressed.

***Hypothesis 2*:** *NPR-A is co-localized with an effector, NKCC1 in the proposed ANP pathway.*

Likely effectors in the proposed ANP pathway will be in extremely close proximity to NPR-A (co-localized). There are several definitions for co-localization, one being expression of the proteins in the same cells, but not overlapping. This manuscript refers to co-localization as the overlap of colors due to expression of the two proteins in the same region of the same cell in the same section (i.e. when yellow label is observed). One potential effector in the ANP pathway is NKCC1, which is located in the stria vascularis and the spiral ligament and acts to transport sodium, potassium, and chloride ions into the endolymph[26]. Using standard immunohistochemical techniques, these experiments looked for the relationship between NPR-A expression and that of NKCC1. Co-localization of the two proteins would implicate NKCC1 as the effector in the ANP pathway, as it would be in such close proximity to NPR-A that it would be logical assume a role in the second messenger cascade.

Experimental Design

These experiments were designed to bridge the gap of knowledge between overlapping observations about the functional role of ANP in the cochlea and the location of its receptor, NPR-A. Without providing a biochemical mechanism, our lab has shown that administering ANP causes a temporary improvement in hearing thresholds[49]

(unpublished). Understanding the location of the receptor proteins is key to determining where ANP may be acting in the cochlea. All experiments were performed on CBA/J mice with normal hearing around 100 days of age. CBA/J mice were used because they do not carry any recessive genes linked to age-related hearing loss[55]. Therefore, CBA/J mice have the most sustainable hearing of any inbred mouse strain.

Two techniques were used to determine the specific location of NPR-A in the cochlea. One of these was immunohistochemistry, which uses antibody staining to visualize the specific location of proteins in a given tissue. The other technique employed was the combination of laser capture microdissection (LCM) and quantitative reverse-transcriptase polymerase chain reaction (qRT-PCR). LCM allows for isolation of specific cells from a tissue. With qRT-PCR, cDNA was generated from extracted RNA and the NPR-A gene was amplified using specific primers to target the gene sequence. Both Immunohistochemistry and LCM/qRT-PCR show the expression of NPR-A in specific tissues and provide information about the location of NPR-A in the cochlea that has not previously been described.

For each hypothesis, it was important to use experimental techniques that could determine the specific location of the desired protein within a given tissue. Immunohistochemistry allows for specific visualization of a chosen protein by using antibodies with precise binding profiles against a particular antigen expressed by the protein. This technique allows researchers to visualize spatial differences of a protein's expression pattern between different tissue types and different samples. Furthermore, by selecting multiple antibodies against different proteins, researchers can observe the

specific relationships between two or more proteins, answering questions about expression patterns and overlapping functions in different tissues.

There are several methods for fine tissue sectioning including cutting in a vibrating microtome, embedding in plastic, or sectioning in a cryostat. Cryostat sectioning was chosen because of its quickness and ease of use. Using a vibrating microtome requires the whole tissue block to be cut, and much more intensive tissue preparation. Embedding in plastic is also a more involved procedure, where as cryosectioning provides a similar product without much difficulty.

Immunohistochemistry involves the use of a primary antibody that is labeled with a secondary antibody containing a fluorescent tag. Alexa fluorescent secondary antibodies were chosen because they are negatively charged and hydrophilic allowing them to stick to tissues better. Additionally, Alexa dyes are more fade resistant than other fluorescent secondary antibodies and produce more vivid colors under microscopy. Alexa fluorescent dyes are also more stable and less pH sensitive than other dyes commonly used in immunofluorescence; this prevents variations in expression levels due to pH manipulations. Alexa fluor®s were chosen in 488 (green) and 568 (red) in order to perform double-labeling experiments to examine the relationship between more than one protein on an individual section.

Complimentary to the immunohistochemical experiments, laser capture microdissection (LCM) was used with quantitative reverse transcriptase polymerase chain reaction (qRT-PCR). LCM allows for the isolation of a particular tissue type from other cells in its native environment. By performing this technique in concert with qRT-

PCR, the mRNA that was actively expressed at the time of collection (an inference to expressed proteins) in a sub-region or cell type (for example cortex vs. medulla of the kidney) were run against the NPR-A primers to determine expression levels. After LCM, the RNA was extracted from the cell isolates, a cDNA copy generated, and PCR run to amplify the NPR-A gene to compare expression levels of NPR-A of specific tissue types within the kidney and cochlea.

Hypothesis 1: NPR-A is located in regions of the cochlea important for the regulation of endolymph ion composition.

1a) Where is NPR-A in the cochlea?

For this portion of the hypothesis, two techniques were used to show NPR-A expression in the cochlea. To determine the location of NPR-A in the cochlea using

Immunohistochemical experiments			
		Antibody 1	Antibody 2
Hypothesis 1: Where is NPRA in the cochlea			
A)	NPR-A in cochlea	Primary: anti-NPRA (Abcam) Secondary: Alexa 568	N/A
		Primary: anti-NPRA (Potter) Secondary: Alexa 568	N/A
B)	NPRA in Intermediate cells	Primary: anti-NPRA Secondary: Alexa 568	Primary: anti-Kir4.1 Secondary: Alexa 488
Hypothesis 2: NPRA and Effectors			
A)	NPRA and NKCC1	Primary: anti-NPRA Secondary: Alexa 568	Primary: anti-NKCC1 Secondary: Alexa 488
Control Experiments			
A)	Positive Control in the kidney	Primary: anti-NPR-A Secondary: Alexa 568	Primary: anti-NKCC1 Secondary: Alexa 488
B)	Negative Control in muscle	Primary: anti-NPR-A Secondary: Alexa 568	Primary: anti-NKCC1 Secondary: Alexa 488

Table 1: Layout of immunohistochemical experiments with corresponding antibodies.
Each immunohistochemical experiment consists of a primary antibody and a secondary antibody. Double labeling of the tissues requires secondary antibodies in different colors in order to determine co-localization. For each experiment, the tissue type is listed (left) with the first label in the middle (primary antibody with corresponding secondary antibody) and the second label on the right. Alexa fluorescent antibodies are listed by color respectively with 568 corresponding to a red wavelength and 488 as a green wavelength. Additionally, Hoechst reagent was added to each secondary antibody dilution to show nuclear material. This reagent was blue in the 405 wavelength. With every experiment, control sections were generated which received no primary antibody labels. This was to reveal any non-specific binding of the secondary antibodies.

immunohistochemistry, two different primary antibodies to target NPR-A were applied on cochlear sections. Anti-NPR-A polyclonal rabbit IgG antibody (Abcam) was tagged with a goat anti-rabbit secondary Alexa fluorescent antibody in red (Invitrogen) using Hoechst to show nuclear material in blue (Table 1). This anti-NPR-A antibody targeted the N-terminal region of the NPR-A protein (amino acids 1-30). Another anti-NPR-A antibody was used, that was developed in the lab of Dr. Lincoln Potter[56]. This was also a rabbit polyclonal IgG antibody, but it targeted the C-terminal region of the NPR-A protein. Both antibodies received the same fluorescent tag and blocking agents (Table 1).

The location of NPR-A in the cochlea was further investigated by qRT-PCR using a forward and reverse primer specific to the NPR-A protein on cells extracted by laser capture microdissection. The primers chosen selected for the NPR-A and GAPDH mRNA (Table 2).

Primers			
Primer	Target Sequence	Base Pair Target	Amplicon Size
NPR-A Left	5'-GTGAAACGTGTGAACCGGAA-3'	2047-2154 bp	108 bases
NPR-A Right	5'-AGCTCCCACAAATCTGGTCA-3'		
GAPDH Forward	5'-AGAACATCATCCCTGCATCC-3'	676-785 bp	110 bases
GAPDH Reverse	5'-CACATTGGGGGTAGGAACAC-3'		

Table 2: Primers and PCR product information.
NPR-A and GAPDH primers (Integrated DNA Technologies) showing base pair targets and amplicon sizes. Amplicon sizes were within the suggested protocols of the Rotor-gene™ kit and all had a GC content of 50%. Additionally, all primers had a melting temperature at approximately 60°C.

The NPR-A primers targeted the 2047th to the 2154th base pairs in the 4065 bp NPR-A gene using the reported sequences (Table 2). This yielded an amplicon of 108

base pairs, a size within the guidelines suggested by the Rotor-gene™ kit, and had a GC content of 50%. Also used were primers for GAPDH, a housekeeping gene. These primers targeted the 676th to the 785th base pairs in the 1275 base pair gene using the reported sequences (Table 2). Both primer sets produced amplicons just above 100 bps; this was confirmed by gel electrophoresis.

1b) Which cells express NPR-A in the stria vascularis?

To determine the expression of NPR-A in the stria vascularis, an antibody specific to intermediate cells of the stria vascularis used in concert with the NPR-A primary antibody to perform a double-label experiment. An anti-Kir4.1 goat polyclonal primary antibody (Santa Cruz Biotech) was used as a marker for intermediate cells of the stria vascularis (as it is only expressed in these cells of the StV (Fig. 2)). This primary antibody was tagged with a chicken anti-goat secondary Alexa fluorescent antibody in green (Table 1). Again Hoechst was used to show nuclear material in blue (Table 1). These experiments were performed as a double label experiment with the NPR-A antibody again in red (as in the individual NPR-A experiments).

Hypothesis 2: NPR-A is co-localized with an effector, NKCC1 in the proposed ANP pathway.

2a) What is the relationship between NPR-A and NKCC1?

Reflecting the larger goals of this study, in addition to determining the specific tissue distribution of NPR-A in the cochlea, it was important to understand its relationship to other proteins that may be involved in the second messenger cascade in the ANP pathway. Because of the relationship of NPR-A to NKCC1 in the renal system

in regards to ion regulation, NKCC1 is a likely candidate for an effector that becomes activated by the NPR-A activation. Anti-NPR-A polyclonal rabbit antibodies (Abcam) were tagged with secondary Alexa fluorescent antibodies against rabbit in red (Invitrogen). Anti-NKCC1 polyclonal goat antibodies (Abcam) were tagged using a green Alexa fluorescent antibody against goat (Table 1) (the same green Alexa fluorescent antibody as in the Kir4.1 double label experiments).

Control Experiments

A) Are NKCC1 and NPR-A in the kidney as reported?

To provide evidence that the primary antibodies against NPR-A and NKCC1 were binding to their antigens as designed, control experiments were performed on tissues other than cochlea. The same antibodies used in the above experiments were used to stain kidney tissue taken from mice after fixation with 4% paraformaldehyde (Table 1). The location of NPR-A[1,57–59] and NKCC1[48,60,61] has been well documented in the kidney and therefore, this experiment acted as a positive control. All experiments used the same dilutions and procedures as the cochlear experiments to ensure comparability. No-primary controls that received the blocking agent during staining were performed to ensure the secondary antibodies were specific to the primary antibodies.

B) Are NKCC1 and NPR-A in muscle tissue?

Again, the same procedures and antibodies as in the cochlear experiments were used on muscle tissue (quadriceps muscle). This experiment acted as a negative control, as neither NPR-A nor NKCC1 have been reported in skeletal muscle. As earlier, no-

primary controls that received the blocking agent during staining were performed to ensure the secondary antibodies were specific to the primary antibodies.

Methods

CBA/J mice were obtained from Jackson laboratories and maintained in the breeding colony at the Duluth campus of The University of Minnesota Medical School. Studies were performed on mice with normal hearing approximately 100 days of age. All procedures were approved by the University of Minnesota Institutional Animal Care and Use Committee.

Tissue Collection and Sectioning

Perfusions

Mice were anesthetized using 0.1 ml of ketamine (2.5 µg/µl)/xylazine (5 µg/µl) anesthesia. Transcardial perfusions were performed in the fume hood on CBA/J mice with a 4% paraformaldehyde, 0.5% picric acid solution for approximately 10 minutes at a rate of 2.6 ml/min. The solution was delivered to the mouse via a 24 gauge, 1-inch needle using an automated, pulsatile pump (Minipuls 2, Gilson Incorporated). To begin the perfusion, the hair covering the chest plate of the mouse was removed. To expose the heart, the thorax was pierced below the lowest rib on the right side and then cut away. The fixative was pumped through the system by inserting the needle into the base of the left ventricle of the heart. Simultaneously, an outlet was created by snipping the right atria to prevent expansion of the tissues and bursting of the membranes during perfusion.

After completion of the perfusion, the kidney and quadriceps muscle were collected as control tissues. These tissues were placed in a series of sucrose dilutions as described in Table 3 in preparation for sectioning. To access the cochlea, the mouse was decapitated, and the skull and brain were removed. The cochleae were then extracted from the skull base and placed in solutions for decalcification and preparation for sectioning (Table 3).

Solution	Time in Solution: Cochleae	Time in Solution: Control tissues
9.3% EDTA	16 hours	n/a
10% Sucrose	10 hours	16 hours
20% Sucrose	14 hours	24 hours
30% Sucrose	24 hours	24 hours

Table 3: Solution timeline for experimental tissues.
Solutions timeline for various tissues after paraformaldehyde perfusion including cochlea, kidney, and the quadriceps muscle. Each tissue was kept in separate jars with both cochlea kept in the same jar. The kidney and muscle tissues did not need decalcification (EDTA) so they were put straight into the 10% sucrose solution.

Cryostat Procedure

A cryostat was used to cut the tissues into fine sections for staining[62]. The tissues were imbedded in OCT media and sectioned at a thickness of 10 μm at -27° C. Sections were collected on Superfrost Plus-one™ charged glass slides, fixed with heat for roughly 5 minutes, and then stored at room temperature overnight in preparation for immunohistochemical staining. Unused sections were then stored at -70° C for future

experiments. Generally the immunohistochemical procedures were performed on freshly fixed tissue to ensure maximum immunoreactivity. However, frozen sections were used as needed and did not show different labeling profiles.

Immunohistochemistry

The sections were first circled using a super PAP™ blocking pen and then incubated in a blocking agent specific to the secondary antibody. For example, anti-Kir4.1 was blocked in 10% normal chicken serum (NCS) because the secondary that was used was raised in a chicken. A summary of antibodies and their blocking agents is shown below (Table 4).

Primary and Secondary Antibodies with Blocking Agents

Primary Antibody	Amino Acid Target	Blocking Agent	Dilution of Primary Antibody	Secondary Antibodies
Anti-NPR-A Rabbit IgG (ab 70848) Abcam	N-terminal	1% Powdered milk in PB	1:50 in block	Alexa 568 Goat anti-Rabbit Invitrogen
Anti-NPR-A Rabbit IgG (Potter) Potter Labs	C-terminal	1% Powdered milk in PBS	1:100 in block	Alexa 568 Goat anti-Rabbit Invitrogen
Anti-NKCC1 Goat IgG (ab 99558) Santa-Cruz Biotechnologies	Internal (aa 769-783)	1% Powdered milk in PB	1:50 in block	Alexa 488 Chicken anti-Goat Invitrogen
Anti-Kir4.1 Goat IgG (sc-23637) Santa-Cruz Biotechnologies	C-terminal	10% Normal Chicken Serum in PBS	1:100 in block	Alexa 488 Chicken anti-Goat Invitrogen

Table 4: Blocking agents with corresponding primary and secondary antibodies. Table showing primary antibodies with their appropriate blocking agents and secondary antibodies. PB is 0.1 M phosphate buffer while PBS is 0.1 M phosphate buffer with saline. Both solutions maintained the same pH of 7.4. Each primary and secondary antibody was diluted in the corresponding blocking agent, an each secondary solution received Hoechst reagent to stain nuclear material (blue). All secondary antibodies were diluted to a 1:200 dilution in the appropriate blocking agent.

Each section was incubated in the blocking agent for 30 minutes. After, the blocking agent was removed, 100 µl/section of the primary antibodies were added and incubated in a humid environment overnight at 4° C. No-primary antibody control sections received the blocking agent during this time period (instead of primary antibody). The second day consisted of 3, 10 minute washes in fresh blocking agent followed by an hour incubation in the secondary antibody at 37.5° C (also in a humid environment). Secondary antibodies were specific to the primary antibody being used to reduce cross-reactivity. Secondary antibodies (Invitrogen) were tagged with either Alexa 488 (green) or Alexa 568 (red). 12.5 µl Hoechst stain was also added to the 1:200 secondary antibody solution and mixed in the blocking agent. Hoechst reagent binds to nuclear material and is in the 405n m range of immunofluorescence, staining all nuclei in blue.

During double label experiments, after 1-hour incubation in secondary antibody, the slides were washed 3 times in 0.1M phosphate buffer (pH 7.4) then submitted to a second round of staining to label the other primary antibody on the same sections (during double label experiments). Again, the procedure was repeated using the blocking agent specific to the primary antibody (Table 4), and a secondary antibody in the other color. Generally, the anti-NKCC1 staining in Alexa 488 chicken anti-goat was performed first,

followed by the anti-NPRA staining in Alexa 568 goat anti-rabbit, but the order did not seem to affect the results.

Imaging

Fluorescent images were taken within a week of staining to ensure accurate depictions of the staining intensities observed. Images were collected using a Zeiss LSM 710 confocal laser-scanning microscope. All images were collected using similar pin hole size, gain, laser power, and pixel lengths to ensure comparability to control sections and between experiments (Table 5).

Confocal parameters	
Pin hole	90
Gain	Between 600-800
Laser power	1.0
Pixel dwell	Between 0.5 to 6 μsec (varied depending on magnification and zoom)

Table 5: Confocal parameters used for section imaging.
All experiments (including control tissues) were imaged using relatively similar settings to ensure comparability among different sections. Natural variability between animals necessitated changes in gain as some sections stained heavily while other sections stained only moderately. Factors influencing this include success of the perfusion, natural protein expression levels, and the cut of the tissue.

Tissue Harvesting

Laser Capture Microdissection

Laser capture microdissection (LCM) involved multiple steps including cryosectioning, dehydration and staining, and capturing of the tissues. The first step, cryosectioning, was performed as described above using similar conditions to the cryosectioning used for the immunohistochemical procedures. LCM was always

performed on fresh tissue, and because the RNA needed to be protected, the slides were kept at -20°C until staining with the Arcturus® Histogene® staining kit. Furthermore, the LCM sections were not heat fixed or air-fixed overnight in order to protect the RNA in the tissues. Cochlear sections were collected on Superfrost™ Excell™ microscope slides while the kidney sections were collected on Histogene® slides provided with the Histogene® staining kit. Cochleae did not adhere well enough to the provided slides, inhibiting the LCM procedure; therefore another slide type was used.

After cryosectioning, the slides were stained using the Arcturus® Histogene® staining kit. Initially, the slides were thawed on a Kim wipe for 30 seconds to warm them to room temperature and adhere the sections to the slides. Following a 30 second dip in 75% ethanol, the slides were hydrated in dH_20 for 30 seconds. On a Kim wipe, the slides were horizontally positioned and the Histogene® stain was added for 20 seconds followed by another 30 second dip in dH_20. Next a series of 30-second emersions in graded ethanols was performed. First, the slides were dipped in 75% ethanol, then 95% ethanol, finalized with 100% ethanol, each for 30 seconds. This dehydrated the sections so that the polymer on the LCM cap would better adhere to the tissue. Lastly, the slides were dipped in xylene for 5 minutes and then air dried in the fume hood for another 5 minutes. To protect the slides, they were stored in a desiccator until LCM was performed (under one hour).

To capture the tissue, the stained slides were blotted with an Arcturus® Prep Strip™ to remove any loose or folded areas and placed on the microscope stage, held in place by the vacuum slide holder. A CapSure® Macro LCM cap was placed on the

placement arm and the sections were examined using the visualizer. Hovering over the tissue, the arm [with cap] was lowered over the tissue to begin microdissection. Proper adhesion to the cap requires the tissue to be flat and dry. Once positioned, the PixCell II™ laser (Arcturus®) was activated with the tracking beam visible on the sections. On a blank patch of slide, the beam was focused and adjusted to a size of 7.5 μm until a sharp edge was seen. Using a laser power of 20 mW for 5 μsec with a focus size of 30 μm, the laser was repeatedly fired over the desired tissue region to pull it from the section. After laser fire, the placement arm with cap was swung off the section and the extracted cells visualized. Before and after pictures were taken to ensure similar size products were captured. To place the cap in the 0.5 mL microcentrifuge tube (RNA/DNAse free) the provided insertion tool was used while allowing for transfer of the cap from the placement arm to the incubation tube without human/glove contact. This protected the RNA samples adhered on the cap from contamination and foreign RNAses. After LCM with a given cap was complete, the cap incubated in the extraction buffer of the PicoPure™ RNA Isolation kit at 42°C for 30 minutes.

LCM was performed on tissues from 8 animals, with only 2 kidney medulla preparations eventually successful at qRT-PCR. None in the cochlea experiments were successful at yielding quality RNA for qRT-PCR. Cochlear sections were extremely hard to capture, most likely because the sections are inherently not flat (a requirement of LCM). Ultimately, just 1 cochlear section yielded captured cells, but the RNA quality was too poor (an issue that will be discussed in a future section) to produce successful qRT-PCR data.

RNA was isolated from specific cell types extracted from the kidney and cochlea using laser capture microdissection (as previously described). Using a PicoPure™ RNA isolation kit (Arcturus), RNA was extracted from individual cell types in both the kidney and the cochlea (Table 6).

Tissue Type	Cell Type
Kidney	Cortex
	Medulla
Cochlea	Spiral Limbus
	Stria Vascularis
	Spiral Ganglion
	Lateral Wall (negative control)

Table 6: Laser capture microdissections from each tissue.
Cochlear dissections were from the entire spiral limbus, a combination of the spiral ligament and stria vascularis, and the lateral wall. Kidney microdissections were from the roughly equal sizes of cortex and medulla. Cochlear extractions were difficult to collect, and only 1 animal of 8 yielded extractable cells.

The LCM caps were incubated in 50 µl of the extraction buffer and heated to 42° C for 30 minutes. After a 2 minute centrifugation at 800 x g, the tubes (with caps) were stored at -80°C until the RNA isolation was performed. The caps were and the provided spin columns were incubated in conditioning buffer at room temperature for 5 minutes, and then spun at 16,000 x g. During the centrifugation, nuclease-free 70% ethanol was added to the RNA samples and gently mixed via pipetting. Multiple cap extractions were combined in one tube to ensure maximum RNA yield. Once the column was prepped with the conditioning buffer, the RNA sample mixture was added. In order to bind RNA to the filter, the tubes were centrifuged for 3 minutes at 100 x g, followed by a 30 second centrifugation at 16,000 x g to remove any liquid in the column. Wash buffer 1 was added to the column, and spun at 8,000 x g for one minute. Following this centrifugation,

wash buffer 2 was added, and the spin column was centrifuged for one minute at 8.000 x g. Another round of wash buffer 2 was performed, spinning at 16,000 x g for two minutes and then again for one more minute. This additional centrifugation ensured all of the wash buffer was removed before RNA elution.

To elute the RNA, the spin filter was transferred to a clean, ½ ml microcentrifuge tube and elution buffer was added to the filter. As instructed by the Arcturus kit, the elution buffer was gently pipetted directly in the filter column. The elution buffer incubated on the filter column for 30 minutes at 42°C to increase the RNA yield. After this incubation, the tube (still containing the filter column) was centrifuged at 1,000 x g to distribute the elution buffer to the filter. A final centrifugation was performed at 16,000 x g for one minute to elute the RNA.

Tissue Homogenates

Homogenate tissue samples were taken from non-perfused animals to test the primer binding and the RT/qPCR procedures. Both kidneys were isolated from 4 animals giving a total of 8 samples. Cochlear homogenate samples were isolated from 3 animals. The samples went through a standard RNA extraction procedure. For kidneys, approximately 80 mg of tissue were used, while whole cochleae were homogenized (naturally mouse cochlea weigh about 15-20 mg each). On the whole, the RNA yields were much higher than the LCM samples, probably because LCM samples went through the sucrose solutions (Table 3) where the RNA had more time to degrade than the fresh tissue from the homogenates. Also, the physical amount of tissue captured via LCM was much less than a homogenate sample.

Quantitative reverse-transcriptase polymerase chain reaction (qRT-PCR) was performed to ensure the unique staining pattern observed in the kidney and cochlea was actually specific to the NPR-A protein (by measuring mRNA levels). After successful RNA isolation, UV spectroscopy (Nanodrop® ND-1000 Spectrophotometer) was performed to approximate the RNA concentration. While this is standard practice for RNA isolation, the PicoPure™ kit notes that these methods may not be reliable for such low levels of RNA. Immediately following this procedure, the samples were either stored at -80°C or kept on ice in preparation for the cDNA generation.

To determine the quality of the RNA, 4 µl samples were sent to the University of Minnesota Genomics Center where a total RNA analysis with picogram sensitivity was performed using a 2100 bioanalyzer from Agilent Technologies Inc. Of the 8 total LCM kidney samples collected (medulla and cortex from each), only 2 registered any RNA present in the sample. Furthermore, cochlear spiral limbus and stria vascularis/spiral ligament samples from the 1 cochlea that was successfully microdissected (CBA 551) were also analyzed, with none yielding quality RNA.

Quantitative Reverse-Transcriptase Polymerase Chain Reaction (qRT-PCR)

Using a QuantiTect® Reverse Transcriptase Kit (QIAGEN), cDNA was generated from the isolated cells pulled from the LCM caps and tissue homogenates. The kit begins with a genomic DNA (gDNA) wipeout reaction. This reaction calls for up to 1 µg of template RNA, as previously estimated by UV spectrophotometry. To complete this reaction, 2 µl of the gDNA wipeout buffer was added to the template RNA and

RNase-free water for a total reaction volume of 14 µl. This reaction was mixed on ice, and incubated in a circulating water bath at 42°C for 2 minutes. During this time, the reverse-transcriptase reaction was prepared using Quantiscript™ reverse transcriptase that contained an RNase inhibitor, Quantiscript RT buffer™ at a 5x concentration that contained Mg^{++} ions and dNTPs, and RT primer mix™. This reaction was mixed with the gDNA reaction mixture and incubated at 42°C for 30 minutes. Once the cDNA was generated, the reaction was immediately added to a 95°C water bath to inactivate the reverse-transcriptase enzyme. The samples were then stored on ice in preparation for the quantitative polymerase chain reaction.

Using the Rotor-gene™ SYBR® Green kit (QIAGEN), the cDNA was run through quantitative polymerase chain reaction (qPCR) to amplify the NPR-A gene. GAPDH (glyceraldehyde 3-phosphate dehydrogenase), an enzyme involved in glycolysis, was also run as a housekeeping gene (as its native to most cells in the body) (Table 2). To perform the reaction, each tube contained 12.5 µl of 2x Rotor-gene™ SYBR® green PCR master mix, 1 µl of each primer (1:4 dilution of both NPR-A or both GAPDH), template cDNA generated using the QuantiTect kit, and RNase-free water for a total reaction volume of 25 µl. Using a Rotor-gene® thermocycler, the entire reaction was preceded with a 5 minute activation step at 95°C. The reaction was set to run 35 cycles of 5 seconds at 95°C to denature and 10 seconds at 60°C for extension and finalized with a melt curve analysis to check the specificity of the primers (Fig. 8).

To confirm the primers were specifically binding to the targeted genes, a number of controls were performed. First, to check that the correct product was being generated,

the PCR product was run on a 2% agarose gel (Fig. 5, left). This confirmed that each amplicon was one product (band) of the targeted size (Table 2). Second, standard curves were constructed to ensure the primers were producing products in a linear range (Fig. 5, right). To generate the standard curves, different dilutions of cDNA were run using the same qPCR conditions as the experimental samples. Essentially, samples with higher DNA concentrations should have higher Ct values than samples with lower amounts of DNA. Standard curves were generated for both the NPR-A and GAPDH primer sets.

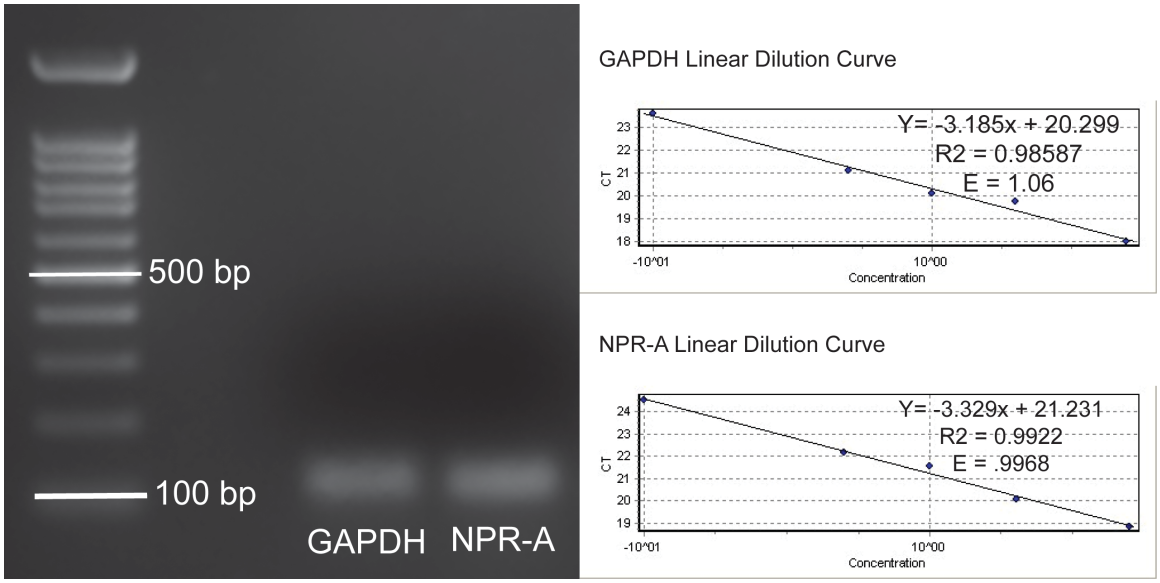

Figure 5: Primer amplicon size and standard curves for GAPDH and NPR-A primers.
Molecular ladder yielding products down to 100 bp were run with qPCR products from GAPDH and NPR-A on a 2% agarose gel. Both samples were from mouse kidney homogenates, CBA 612. Standard curves for the GAPDH (top right) and NPR-A (bottom right) primer sets showing the linear dilution curves for cDNA.

Lastly, qPCR products were sent for sequencing to ensure the correct genes were amplified. GoTaq® Green master mix was substituted for the 2x Rotor-gene™ SYBR® green PCR master mix and does not produce fluorescence during qPCR. The products were gel extracted and run through a PCR clean up procedure in preparation for

sequencing. This cDNA reaction was doubled from the standard 25 µl reaction to the 50 µl to ensure enough product was made. The reactions were run through the standard qPCR run, without the final melt step. 25 µl of both the NPR-A and GAPDH products were run on a 2% agarose gel to visualize the amplicon. Using standard kits, the gel products (both just over 100 bps) were extracted and melted, then run through the gel extraction kit. These products were re-combined with the other half of the GoTaq® Green master mix product and run through a standard PCR clean up kit. In preparation for sequencing, 12 µl of the product were combined with 1 µl of one diluted primer (4 tubes in total, 1 for each primer) and sent to the University of Minnesota Genomics Center for DNA sequencing. Of the 4 primer tests sent, both NPR-A primers and the GAPDH reverse primer yielded the correct product. The DNA yields were low after PCR clean up, which may have caused the failure of the forward GAPDH primer.

To analyze the qPCR results, raw Ct values were obtained from the Rotor-Gene™ software. Only 1 run of each homogenate sample was performed, but for the LCM samples, Ct values from multiple runs were averaged for the following calculations. From the Ct values, mRNA concentrations were calculated using the linear regression equations from the standard curves for each primer set, and used to compute the ratio of the absolute NPR-A expression levels to the absolute GAPDH expression levels. The relative expression of NPR-A to GAPDH mRNA concentration for each tissue [cochlear homogenates, kidney homogenates, and kidney medulla LCM] was determined (Fig. 9).

Results

The results of these experiments provided novel information about the location of NPR-A in the cochlea, as well as its relationship to other proteins such as Kir4.1 and NKCC1. NPR-A was found in regions of the cochlea critical to K^+ recycling and fluid balance. These areas included the root cells of the spiral ligament, interdental cells of the spiral limbus, and cells of the stria vascularis. NPR-A was also found in spiral ganglion neurons pointing to its role in neurotransmission. NKCC1 was found in the spiral ligament, where it did not co-localize with NPR-A. NKCC1 did intermittently co-localize with NPR-A in other regions such as the stria vascularis and the spiral limbus. NKCC1 did not label the spiral ganglion neurons. Both antibodies labeled the tectorial membrane.

Control Experiments

Kidney and muscle samples served as positive and negative controls respectively for both NPR-A and NKCC1. The heaviest NPR-A labeling was in the tubules and renal podocytes (glomeruli) of the cortex, although these techniques did not allow for differentiation between various tubules and collecting ducts (Fig. 6d). NPR-A label was also observed in the blood vessels associated with the renal cortex (Fig. 6f). Additionally, some staining was observed in the medulla (Fig. 6e). This labeling is consistent with previous reports of NPR-A expression in renal podocytes, blood vessels, tubules and collecting ducts[63–65]. Analyzing our NKCC1 label, there was heavier staining

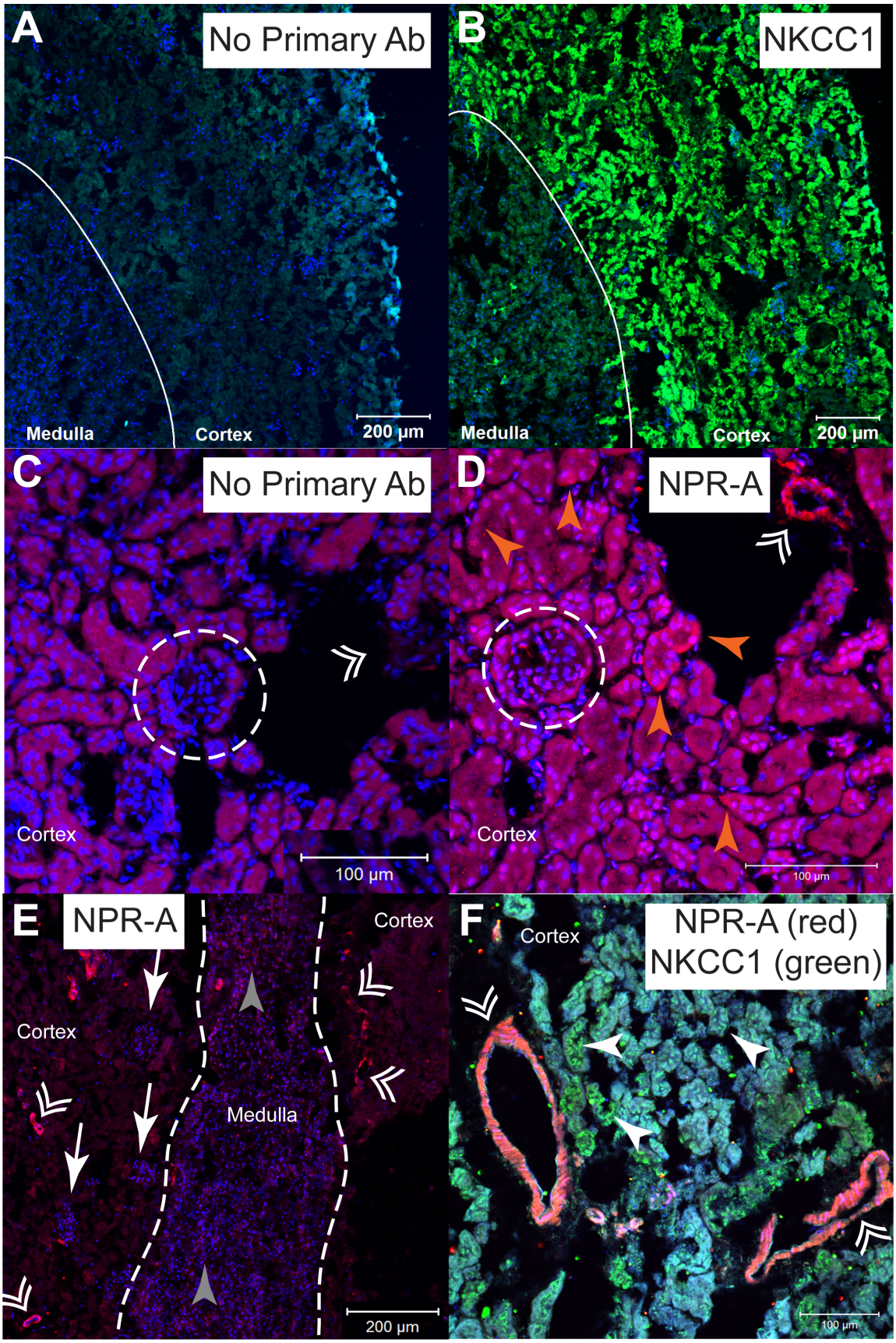
A
No Primary Ab
Medulla
Cortex
200 µm
B
NKCC1
Medulla
Cortex
200 µm
C
No Primary Ab
Cortex
100 µm
D
NPR-A
Cortex
100 µm
E
NPR-A
Cortex
Cortex
Medulla
200 µm
F
Cortex
NPR-A (red)
NKCC1 (green)
100 µm

Figure 6: Positive controls showing NPR-A and NKCC1 expression in the kidney. A-B. Mouse kidney cross-sections from CBA 505. A. Control image with no primary antibody. B. Experimental image with anti-NKCC1 (Abcam) with an Alexa fluor 488 in green showing NKCC1 expression in both the medulla and cortex. C. Control image of CBA 532 cortex with no primary antibody. D. Experimental image of CBA 532 cortex with anti-NPR-A (Abcam) labeled with Alexa 568 in red showing NPR-A expression in tubules (orange arrowheads), glomeruli (circled), and renal blood vessels (double arrowheads). E. Experimental image from CBA 505 showing both the cortex and medulla (outlined). NPR-A expression was in renal blood vessels (double arrowheads), and areas of the medulla (grey arrowheads). F. CBA 521 kidney cortex double-labeled with NPR-A and NKCC1. NKCC1 expressing in tubules/collecting ducts (white arrowheads) and NPR-A expression in blood vessels (double arrowheads). Note NPR-A was also expressed in tubules, but this was overshadowed by the green label of NKCC1 in double label images.

in the cortex of the kidney with less staining in the medulla (Fig. 6b). These results are also consistent with previous reports about NKCC1 expression in the kidney.

The quadriceps muscle acted as a negative control because neither NKCC1 nor NPR-A have been reported in skeletal muscle[66,67]. Neither protein was significantly expressed (Fig. 7).

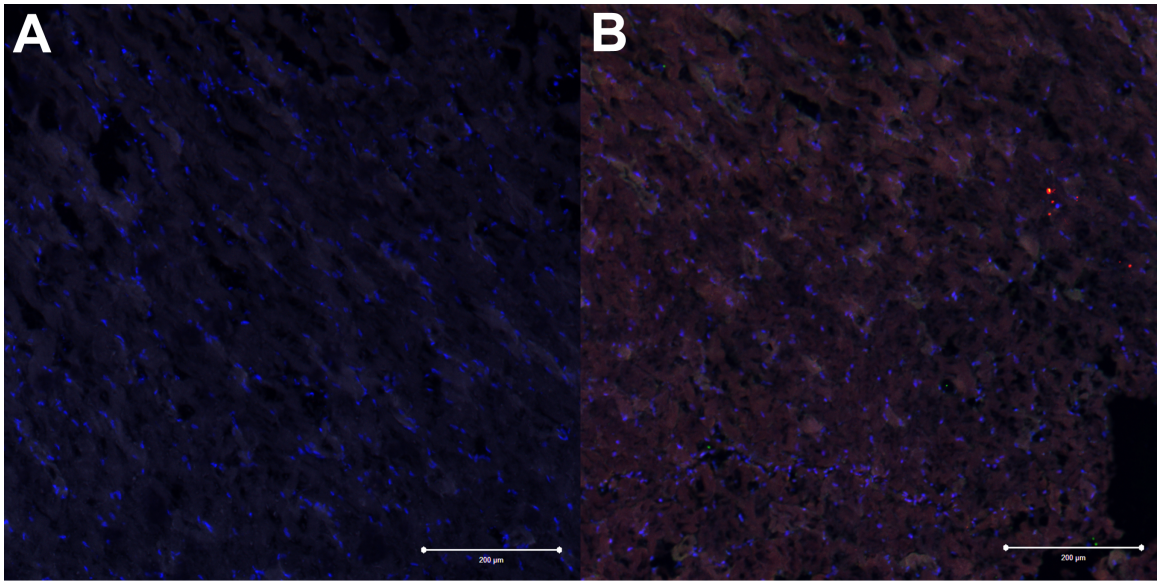

Figure 7: Negative controls showing lack of NPR-A and NKCC1 expression in muscle tissue.
Mouse muscle from CBA 518. A. Control image with no primary antibodies. B. Experimental double-label image with NPR-A in red and NKCC1 in green. Both images show Hoechst reagent in blue indicating the presence of all cells. Sections were taken from the quadriceps muscle of mice fixed with paraformaldehyde (same conditions as cochlear staining). Note relative similarity between the control (A) image and experimental image (B). NKCC1 and NPR-A have not been reported in skeletal muscle, and therefore the lack of staining indicates the primary antibodies are not binding to regions that do not express those proteins.

Laser capture and qRT-PCR

Using the NPR-A and GAPDH primers, melt curves were produced, revealing binding of the primers to the cDNA gene template. As shown (Fig. 8), cochlea and kidney homogenate samples, as well as LCM kidney medulla samples expressed NPR-A and GAPDH. The 2 LCM samples that showed measurable bands from the RNA analysis were also the samples that produced amplicons during qPCR, as evident by clean and distinct melt curves. These samples were also only from medulla, as none of the cortex samples produced enough RNA to generate a melt curve. However, based on both the immunohistochemical results and the literature, kidney cortex does express NPR-A, so this observation was most likely due to the low quality/amount of RNA yield. Additionally, there were some LCM samples that did show GAPDH reactions in both the medulla and cortex (data not shown).

There was no significant difference in NPR-A expression between the cochlea and kidney homogenates relative to GAPDH ($p = 0.50265$, 2 sample t-test) (Fig. 9). For the LCM medulla samples, mRNA recovery appeared to give qualitatively similar NPR-A levels as kidney homogenates, although this observation is purely correlative ($n = 2$).

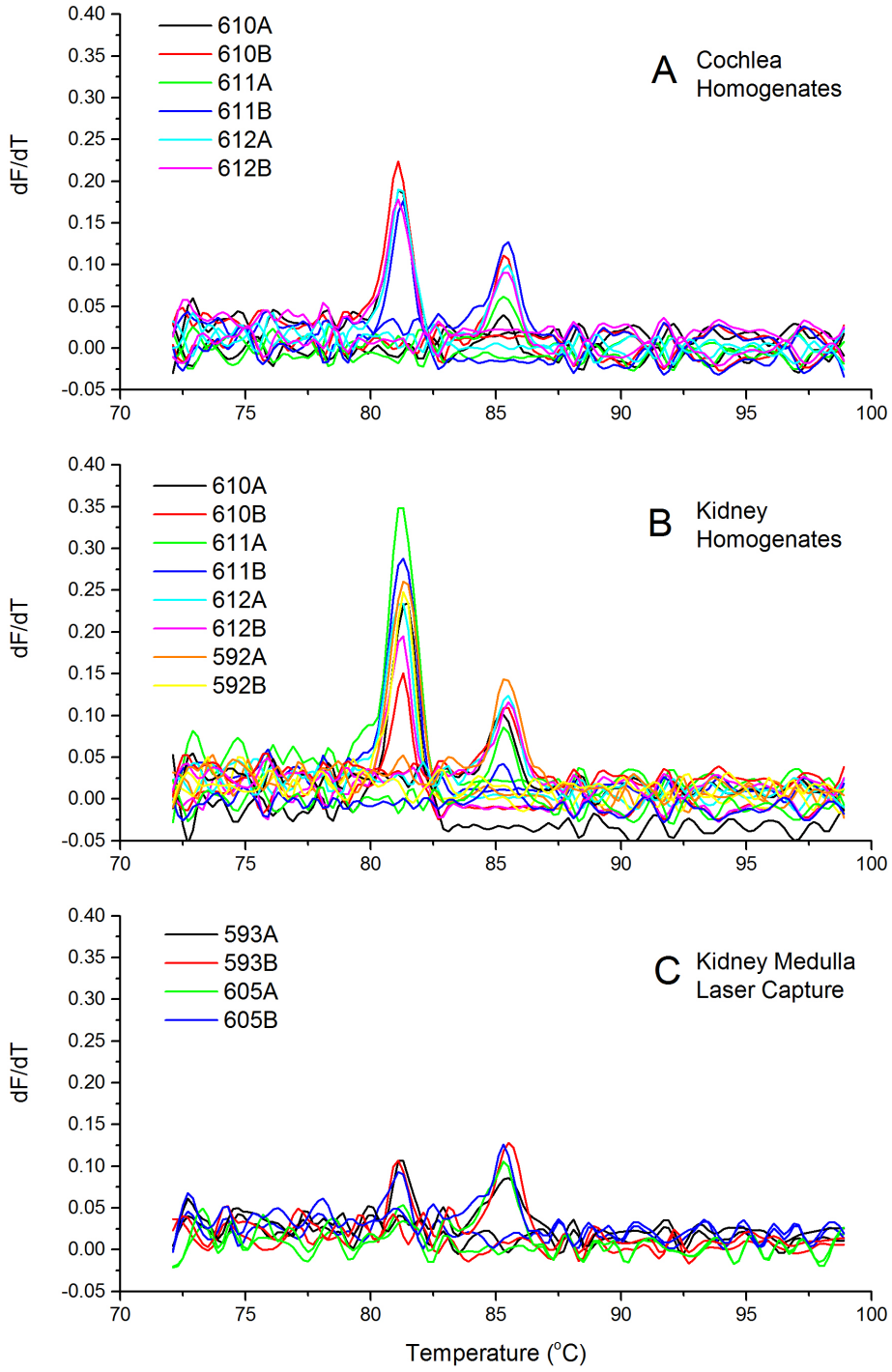
A
Cochlea
Homogenates
610A
610B
611A
611B
612A
612B
B
Kidney
Homogenates
610A
610B
611A
611B
612A
612B
592A
592B
C
Kidney Medulla
Laser Capture
593A
593B
605A
605B
dF/dT
Temperature (°C)

Figure 8: Melt curve analysis from kidney and cochlea homogenate and LCM kidney medulla samples.
Melt curve analyses show that only one peak was generated for each primer set in all samples. In each panel, the left peak corresponds to the NPR-A primer set and the right peak to the GAPDH. A. Cochlea homogenates from 6 samples (611A did not produce an NPR-A melt curve, and only had a low GAPDH peak). B. Kidney homogenates from 8 total kidneys, 4 separate animals. C. LCM samples from kidney medullas in two animals. Samples from 6 other animals were run, but only these 2 yielded successful NPR-A melt curves.

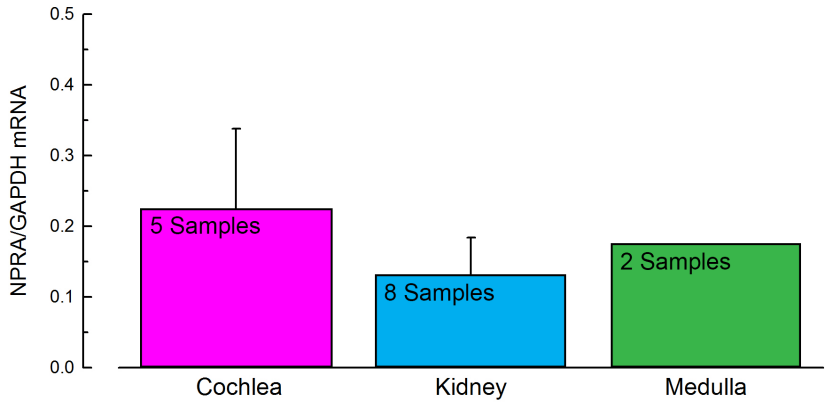

Figure 9: Relative expression of NPR-A to GAPDH in three unique tissue samples.
Values for each peak were calculated using the linear regression from the standard curves for each primer set. This graph represents the difference in relative expression of NPR-A to GAPDH absolute values (see methods). The medulla peak does not have a standard error bar as it was composed of only 2 samples and statistical calculations were not applicable.

Hypothesis 1: NPR-A is located in regions of the cochlea important for the regulation of endolymphatic ion composition.

1a) Where is NPR-A in the cochlea?

Using fluorescent immunohistochemistry and confocal microscopy, NPR-A was found in multiple tissue types of the cochlea (Fig. 10). These tissue types included type I spiral ganglion cells (1), interdental cells of the spiral limbus (2), root cells of the spiral

ligament (3), and several cells of the stria vascularis (4) (Fig. 10). No differences were noted between the basal and apical turns of the cochlea.

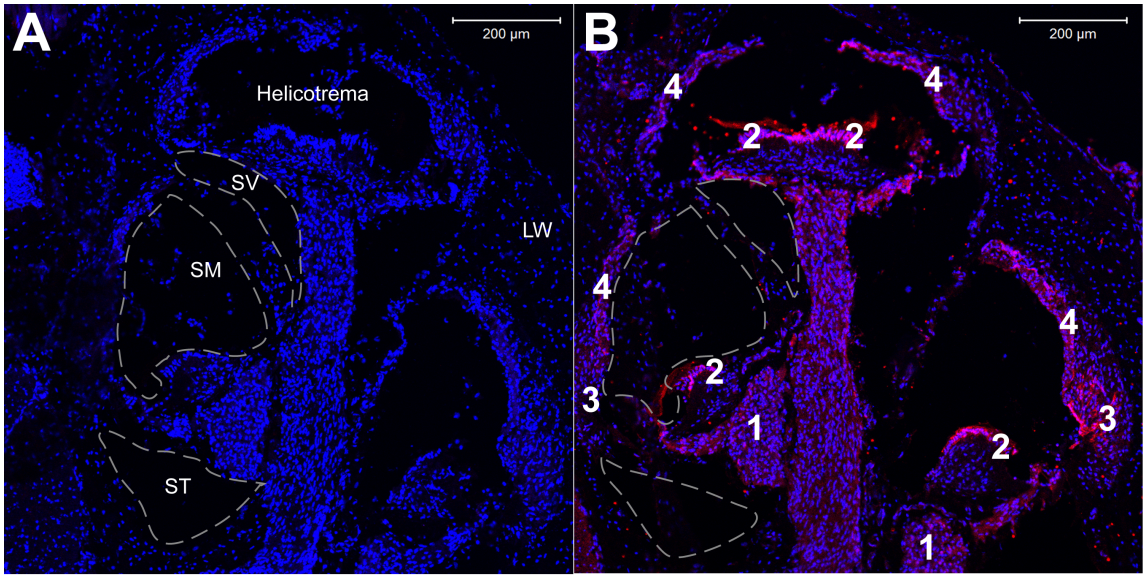

Figure 10: NPR-A was found in four specific regions of the cochlea.
Mouse cochlea of CBA 432 showing the 1.5 turns of the scalae in cross section. A. Control image with no primary antibody. B. Experimental image with anti-NPR-A primary antibody. Both sections were exposed to a secondary antibody of Alexa 568 goat anti-rabbit (red) and Hoechst reagent (blue). Positive staining was found in 4 distinct areas including the (1) cell bodies and central/peripheral processes of the spiral ganglion, (2) interdental cells of the spiral limbus, (3) root cells of the spiral ligament, and (4) cells in the stria vascularis. SV Scala vestibuli. SM Scala media. ST Scala tympani. LW lateral wall.

Spiral ganglion

The spiral ganglion contains the cell bodies of the nerve fibers that travel from the hair cells into the modiolus of the cochlea to form the vestibulocochlear nerve. NPR-A was found in both the cell bodies of the spiral ganglion and the central and peripheral projections (Figs. 10 and Fig. 11). However, NPR-A was not found within the hair cells themselves, but only in the tectorial membrane. Most of the label observed in the organ of Corti was of the nerve terminals of the peripheral processes. NPR-A expression was

specific only to Type I spiral ganglion neurons and not found in the cell bodies found along the outside of the ganglion (the type II neurons). NPR-A was also noted in the peripheral processes that communicate with inner hair cells (type I neurons), but was not noted crossing the basilar membrane and therefore not expressed in peripheral processes that communicate with outer hair cells (Type II spiral ganglion neurons).

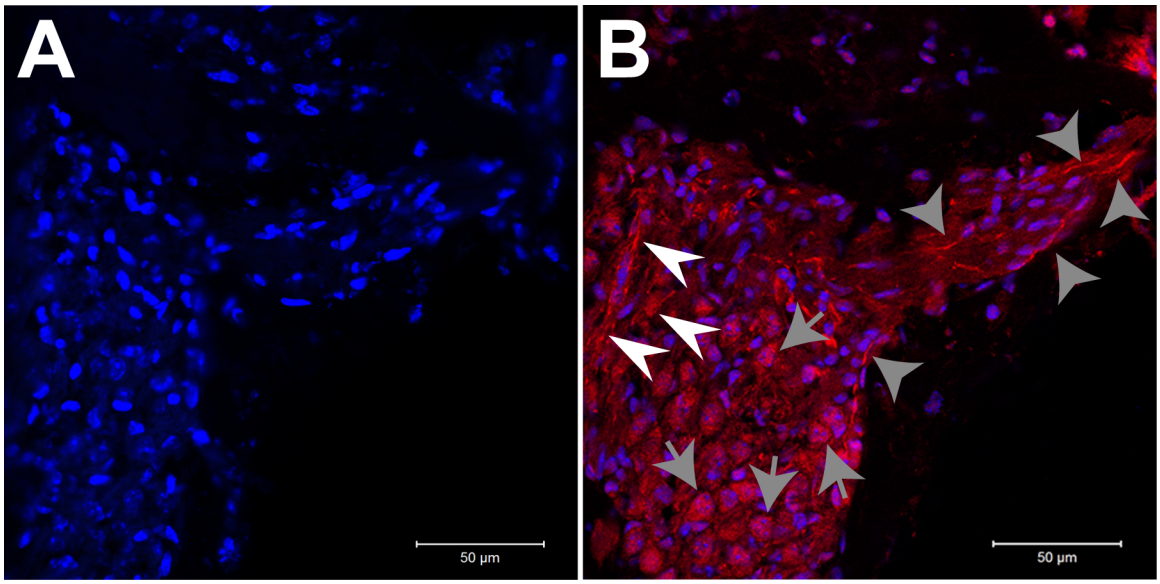

Figure 11: NPR-A was expressed in nervous tissue of the spiral ganglion.
Mouse spiral ganglion cells. A. Control image from CBA 596 with no primary antibody. B. Experimental image from CBA 518 with anti-NPR-A primary antibody. Both sections used a secondary antibody Alexa 568 goat anti-rabbit (red) label and Hoechst reagent (blue). The expression pattern of NPR-A was specific to the neurons and was not present in the surrounding boney tissue of the modiolus or the supporting cells. Arrows in B indicate the expression of NPR-A in the cell bodies of Type I spiral ganglion cells (grey arrows), the peripheral processes heading towards the hair cells (grey arrowheads), and central processes heading towards the auditory nerve bundle in the modiolus (white arrowheads).

Spiral Limbus

NPR-A was expressed in the interdental cells that line the scala media (Fig. 12), including all three sub-types. These cells are apically exposed to endolymph and act as an exit point for K^+ from the epithelial gap-junction network (Fig. 1). NPR-A expression

was localized to the entire cell body of the interdental cells, and not just one cellular pole. There was little staining in the other areas of the spiral limbus using the N-terminal antibody (Abcam). Occasionally, slight staining was observed in the inner sulcus cells. However, this staining was much less bright and obvious than the staining within the interdental cells (Fig. 12). As described by Spicer and Schulte (1998), the spiral limbus has three interdental cell types and two fibrocyte types[11]. These N-terminal antibody stained all 5 of these subtypes, although no molecular marker was used to differentiate among the limbal subtypes.

Spiral Ligament

In the spiral ligament, NPR-A was found only in the root cells, and not expressed in any of the surrounding fibrocytes (Fig. 13). Root cells line the curve of the membranous portion of the lateral wall (the outer sulcus), covering the transition from the basilar membrane to the spiral ligament proper. These cells are apically exposed to endolymph, and have basolateral projections deep into the fibrocyte network of the spiral ligament[18]. NPR-A specifically stained in both the cell body and root processes, being present throughout the entire cell.

C-terminal (Potter) Antibody Staining

Similar expression patterns were observed between the N-terminal (Abcam) and C-terminal (Potter) antibody labels, although there were some variances in intensities (Fig. 14). The only major difference was in the staining of the spiral limbus, where the C-terminal (Potter) antibody exhibited staining in limbal fibrocytes as well as the

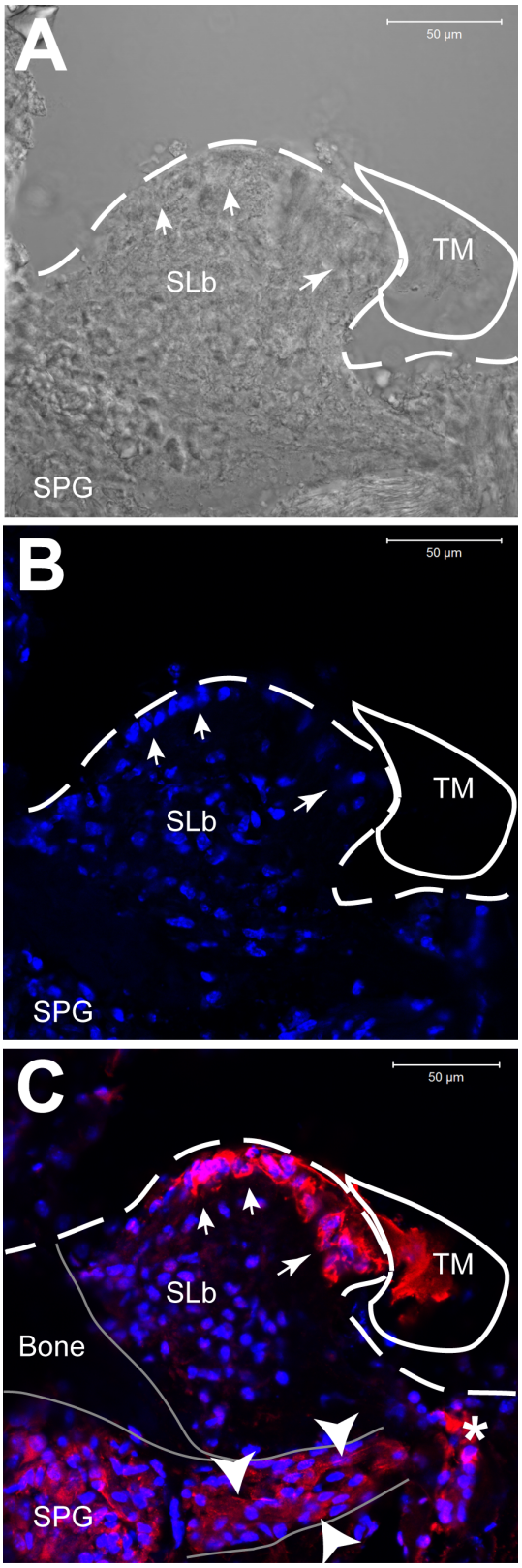

Figure 12: NPR-A was expressed in interdental cells of the spiral limbus. Sections from the spiral limbus in the mouse cochlea of CBA 596. Arrows indicate the interdental cells in each panel. A. Transmitted light image showing the spiral limbus tissue. B. Control image with no primary antibody. C. Experimental image with anti-NPR-A primary antibody. All treatments have a secondary antibody of Alexa 568 goat anti-rabbit (red) and Hoechst reagent (blue). Note the outline around the tectorial membrane in each image, which is not stained when the primary antibody is not present (B). Interdental cells are indicated with white arrows, with limbal fibrocytes acting to support them. NPR-A was also expressed in the spiral ganglion (C) in both the cell bodies and peripheral processes that travel through Rosenthal's canal towards the inner hair cells (arrowheads). Possible label in the terminal buds of the neurons was also observed (asterisk). SLb spiral limbus. SPG Spiral ganglion. TM Tectorial membrane.

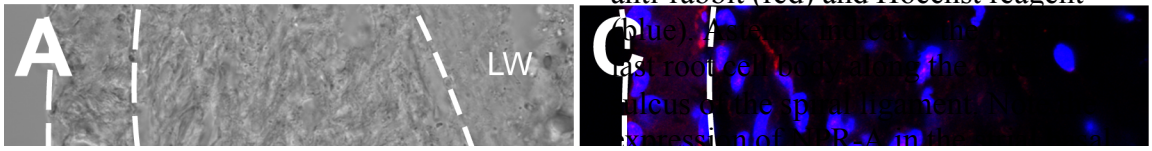

Figure 13: NPR-A was in the root cells of the spiral ligament.
Images of the spiral ligament from mouse cochlea. A. Transmitted light image showing the spiral ligament tissue from CBA 596. B. Control image with no primary antibody from CBA 596. C. Experimental image with anti-NPR-A primary antibody (red) from CBA 432. Note the intense expression pattern of NPR-A deep within the spiral ligament. (B/C) Both sections have a secondary antibody of Alexa 568 goat anti-rabbit (red) and Hoechst reagent

interdental cells as seen with the N-terminal (Abcam) antibody (Fig. 12). The specific locations and degree of labeling observed with the two NPR-A antibodies are summarized (Table 7). Due to the complicated morphology and expression patterns in the strial vascularis, they will be discussed in a later section.

Tissue type	NPR-A Staining (Abcam)	NPR-A Staining (Potter)	Cell Type
Spiral limbus			Connective
Interdental cells	+++	++	
Fibrocytes	-	++	
Stria Vascularis			Epithelial
Marginal cells	++	+	
Intermediate cells	-	-	
Basal cells	+++	+	
Spiral ligament			Connective
Root cells	+++	++	
Fibrocytes	-	-	
Spiral ganglion	+++	++	Nervous
Tectorial membrane	+	+	Connective
Organ of Corti			
Hair cells	-	-	Sensory
Supporting cells	-	-	Epithelial
Basilar membrane	-	-	Connective
Reissner's membrane	-	-	Connective
Lateral wall	-	-	Bone
Modiolus	-	-	Bone

Table 7: NPR-A was in regions of the cochlea specific to potassium recycling and neurotransmission.
Specific tissue locations of NPR-A within the cochlea using two antibodies against different regions of the protein. (+) denotes positive staining, with degree represented by number of signs. (-) indicates negative staining. Last column lists cell types of each tissue listed. Staining was occasionally observed in connective tissue such as the basilar and tectorial membranes, but not always observed.

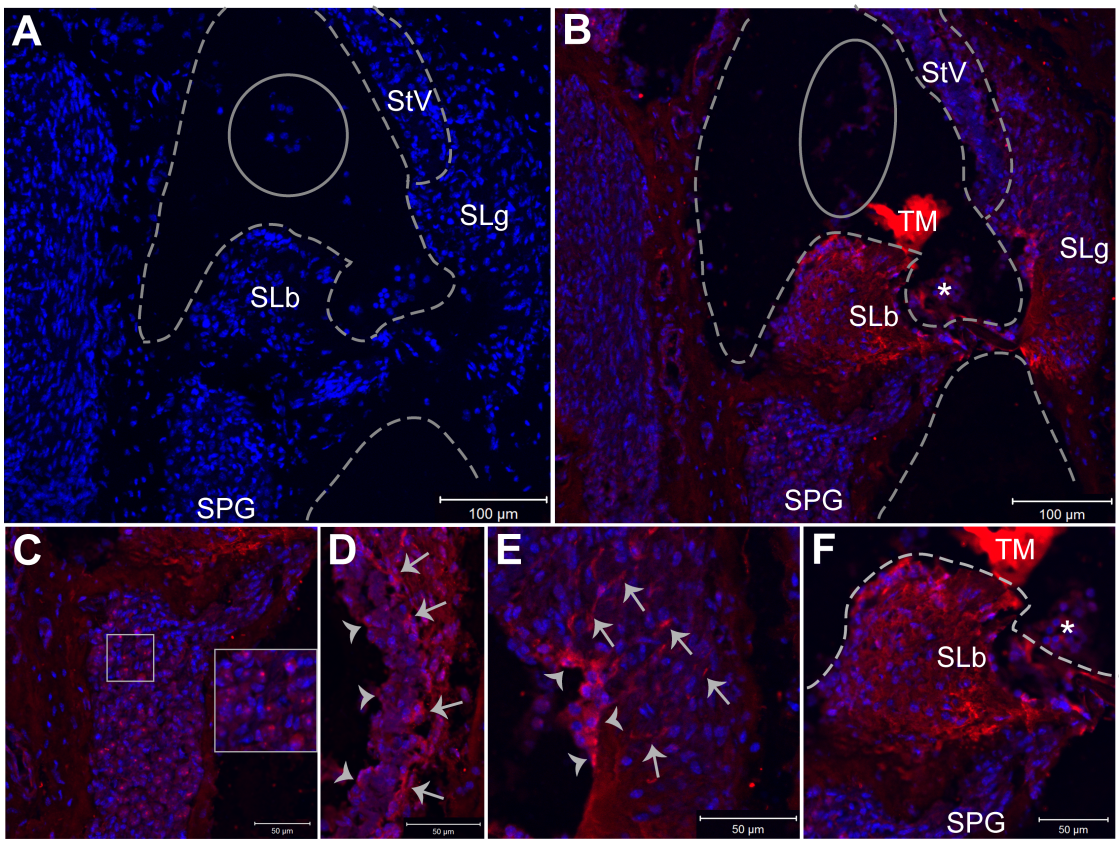

Figure 14: NPR-A expression in the cochlea using the Potter antibody.
A-F. CBA 518, 1:100 C-terminal antibody (Potter) against NPR-A. Similar expression patterns to the N-terminal NPR-A antibody (Abcam) were observed. All sections used a 1:200 secondary antibody Alexa 568 (red) goat anti-rabbit label and Hoechst reagent (blue). A-B. Grey circle for the collapsed cells of Reissner's membrane with different scalae outlined with doted lines. A. Control image with no primary antibody. B. Experimental image showing NPR-A expression in the spiral limbus (SLb), spiral ganglion (SPG), spiral ligament (SLg), and stria vascularis (StV). Expression also noted in the tectorial membrane (TM). Asterisk indicates the organ of Corti. C. Mouse spiral ganglion showing expression in both the cell bodies and central and peripheral processes of the nerve cells. Insert shows cropped image spiral ganglion cell bodies with NPR-A expression. D. Mouse stria vascularis with marginal cell (arrowheads) and basal cell (arrows) NPR-A expression. E. NPR-A expression in the cell bodies of the root cells of the spiral ligament (arrowheads) and their lateral projections (arrows). F. Experimental image showing the NPR-A expression in the spiral limbus (outlined). NPR-A was expressed in interdental cells as well as limbal fibrocytes. Note the non-specific staining in the tectorial membrane as well as the slight stain in the collapsed cells of the organ of Corti (asterisk).

A similar expression pattern was observed using both antibodies, although disparities in intensity were observed, as well as the differences in expression in the spiral limbus. The dissimilarity of the two antibodies in the stria vascularis was not due to cellular localization, but was specific to the intensity of the stain. Using the C-terminal antibody, both basal and marginal cells did not stain as vividly but label was clearly observed. The N-terminal antibody (Abcam) staining was much stronger, but again was still found in the same areas as the C-terminal antibody. Other regions in the cochlea did not show differences in staining using the two NPR-A antibodies.

Stria vascularis

NPR-A labeling was evident in the stria vascularis (Figures 10, 13, and 14). NPR-A was expressed along the basal pole of the basal cells as well as throughout the body of the marginal cells. There was variability in the staining intensity with both NPR-A antibodies noted within the intermediate layer of the stria vascularis, which made it unclear whether NPR-A was local only to marginal cells [and their projections] or within the intermediate cells themselves (that are interdigitated among the MC projections). In order to determine the specific strial cell types that express NPR-A, the second portion of the hypothesis was developed.

1b) Which cells express NPR-A in the stria vascularis?

Because Kir4.1 is only expressed in the intermediate cells of the stria vascularis[29], dual labeling with NPR-A was employed to determine whether NPR-A labeling was specific to this cell population in the stria vascularis. Co-localization between NPR-A

and Kir4.1 (Fig. 15) was not observed suggesting that NPR-A was in the basolateral projections of marginal cells and not in the intermediate cells.

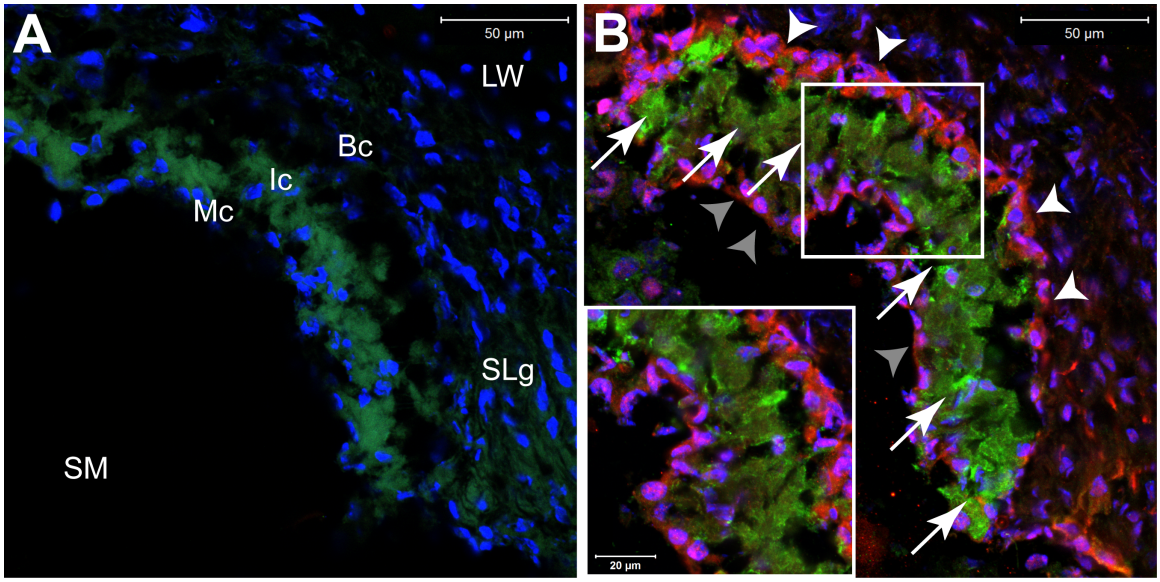

Figure 15: NPR-A and Kir4.1 did not co-localize in the intermediate cells of the stria vascularis.
Stria vascularis of the mouse cochlea from CBA 521. A. Control image with no primary antibodies. B. Experimental double-label image with anti-Kir4.1 (green) and anti-NPR-A (red) with Hoechst reagent (blue). No co-localization was observed, indicating NPR-A was not expressed in intermediate cells (white arrows), with any label in that area attributed to projections from the abutting marginal cells (grey arrowheads) or basal cells (white arrow heads). While the control image (A) showed low levels of green label, this was due slight non-specific binding of the secondary antibody (specific green label in B noted with white arrows). Inset shows the mid section of the stria vascularis. Note the red stain and green strain in the "middle" of the stria vascularis, lacking any yellow overlap.

To summarize, NPR-A was found in four distinct regions of the cochlea including the stria vascularis, the spiral ligament, spiral limbus, and spiral ganglion. Using both the N-terminal (Abcam) and C-terminal (Potter) antibodies along with the double-labeling experiments of NPR-A with Kir4.1, NPR-A was in the marginal cells of the stria vascularis and the basal portion of the basal cells within the stria vascularis. Looking at the spiral ligament, NPR-A was localized to the cell bodies and root processes of the root

cells, but not expressed in the surrounding fibrocytes. Expression within the spiral ganglion showed NPR-A in the cell bodies and central/peripheral processes of Type I spiral ganglion cells, but not in the Type II spiral ganglion cells or Schwann cells. Lastly, NPR-A was expressed in the interdental cells of the spiral limbus (both antibodies) and the limbal fibrocytes (C-terminal antibody) as summarized (Fig. 16).

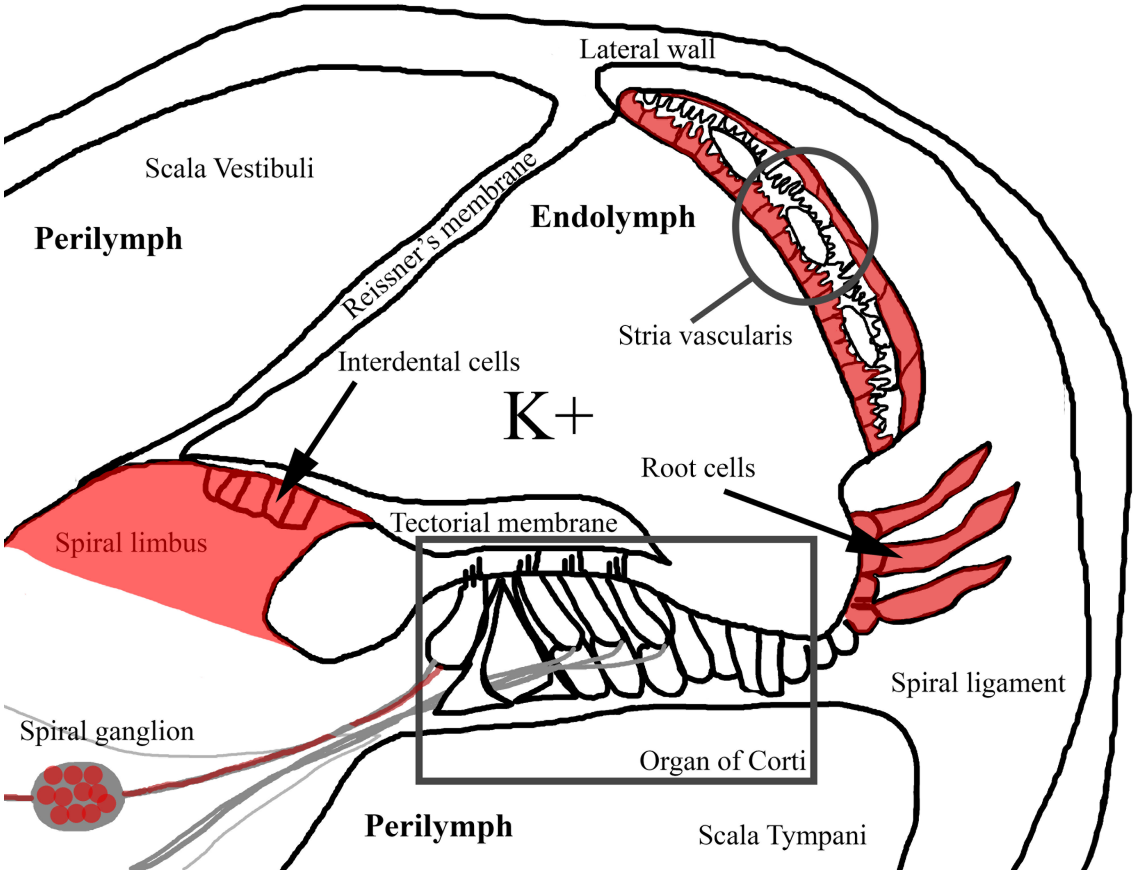

Figure 16: NPR-A expression in the cochlea.
Summary diagram of the expression of NPR-A in the cochlea showing the specific regions positive for NPR-A labeling. NPR-A was found in the marginal and basal cells of the stria vascularis, root cells of the spiral ligament, interdental cells (and limbal fibrocytes) of the spiral limbus, and spiral ganglion neurons. Some label was also observed in the tectorial membrane.

Hypothesis 2: NPR-A is co-localized with an effector, NKCC1 in the proposed ANP pathway.

2a) What is the relationship between NPR-A and NKCC1?

NKCC1 was expressed in the stria vascularis, spiral ligament, and spiral limbus (Table 8). The relationship between NPR-A and NKCC1 was complex, in that some tissues showed co-localization, some showed segregated expression, and some NPR-A containing regions did not express NKCC1 at all (Table 8). As previously stated, this thesis regards co-localization as any yellow color observed, theoretically due to the expression of both proteins in the same region of the same cell at the same time [co-localization could also mean just in the same cell]. The spiral limbus contained the highest degree of co-localization, as interdental cells expressed both NPR-A and NKCC1. Moreover, there was some intermittent co-localization in some cells of the stria vascularis, however this was infrequent.

Spiral limbus

Within the spiral limbus, NKCC1 was expressed more medially away from the inner sulcus. NKCC1 was expressed in interdental cells and in central and medial limbal fibrocytes (Fig. 17). However, NKCC1 and NPR-A intermittently co-localized within the interdental cells (both antibodies). While this co-localization was often observed, it was not ubiquitous to every cell nor was it observed in every animal (Fig. 17). For example, the spiral limbus shown in figure 18b shows less co-localization in the interdental cells than is shown in figure 17. Co-localization was not observed in limbal fibrocytes using

Tissue type	NPR-A Staining	NKCC1 Staining (Abcam)
Spiral limbus		
Interdental cells	+++	++
Limbal fibrocytes	-(Abcam)/++(Potter)	++
Stria vascularis		
Marginal cells	+++	++
Intermediate cells	-	-
Basal cells	+++	-
Spiral ligament		
Root cells	+++	-
Fibrocytes	-	++
Spiral ganglion	++	-
Tectorial membrane	++	++
Organ of Corti		
Hair cells	-	-
Supporting cells	-	-
Basilar membrane	-	-
Reissner's membrane	-	-
Lateral wall	-	-
Modiolus	-	-

Table 8: Summary of expression patterns of NPR-A and NKCC1 within the cochlea. NPR-A and NKCC1 were often expressed in similar regions of the cochlea, but rarely exhibited co-localization. NPR-A and NKCC1 intermittently co-localized in the interdental cells of the spiral limbus and the basolateral surface of the marginal cells in the stria vascularis. NPR-A and NKCC1 did not co-localize in the basal cells of the stria vascularis or the spiral ligament. NKCC1 was not expressed in the spiral ganglion. (+) denotes positive staining, with degree represented by number of signs. (-) indicates negative staining.

both the N-terminal antibody (Abcam) (Fig. 17) and the C-terminal antibody (Potter) (data not shown).

Stria vascularis

NKCC1 was expressed in the most medial layer of the stria vascularis, consistent with earlier observations that NKCC1 is found in the basolateral plasmalemma of the marginal cells in the StV[20]. NPR-A and NKCC1 did co-localize in the marginal cell layer

in an intermittent expression pattern similar to the observations in the interdental cells of the spiral limbus (Fig. 18). NKCC1 was expressed with less intensity through the intermediate cell layer of the StV, and was not found in the basal cells. Staining was also observed abutting the basal cells, however this was likely due to the marginal cell projections, which extend all the way to the basal cells (Fig. 18c-e).

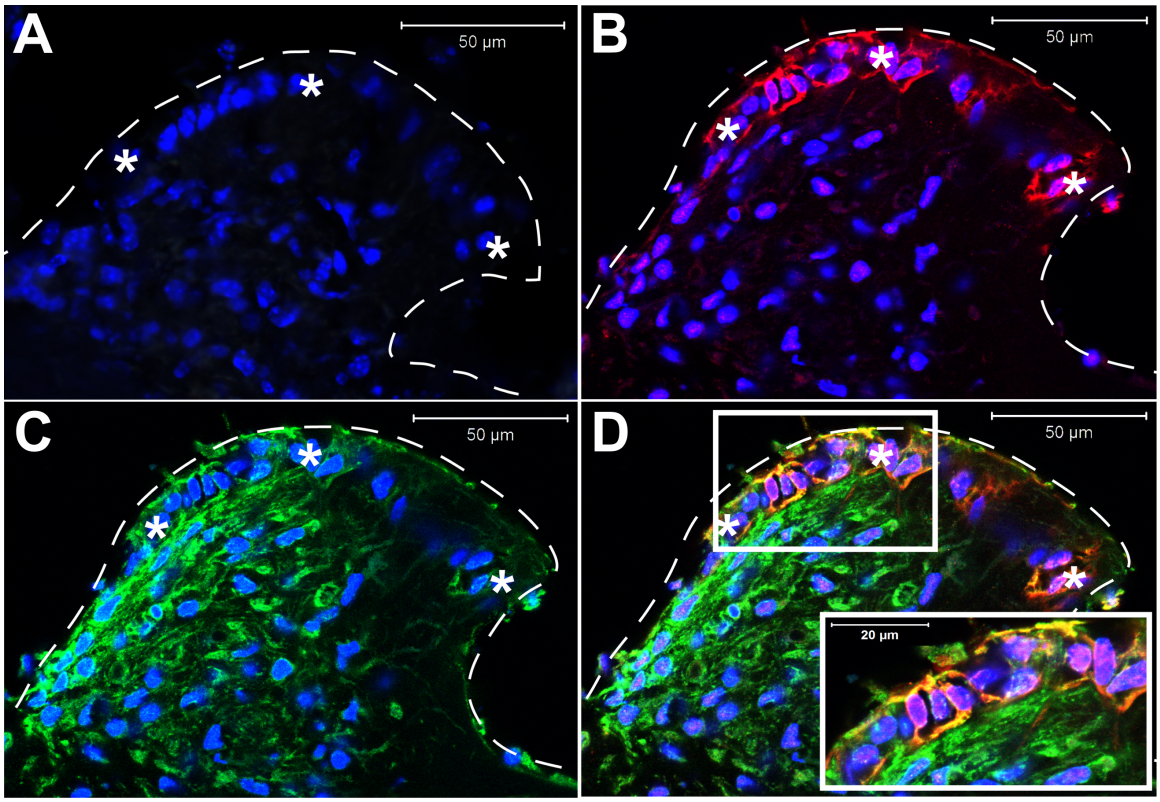

Figure 17: Slight co-localization pattern of NPR-A and NKCC1 in the spiral limbus. Spiral limbus sections from the mouse cochlea. A. Control image from CBA 297 with no primary antibodies. B. Experimental image with anti-NPR-A primary antibody with secondary Alexa 568 (red). C. Experimental image with anti-NKCC1 with the secondary Alexa 488 (green). Both images have Hoechst reagent (blue). D. Merged image from CBA 432 of the two secondary labels where yellow indicates regions of co-localization of the two proteins. Note the asterisk highlighting examples of the location of interdental cells on the endolymphatic surface of the spiral limbus. Inset shows specific interdental cells positive for both NPR-A and NKCC1 expression (yellow), with some exhibiting only one protein (green or red).

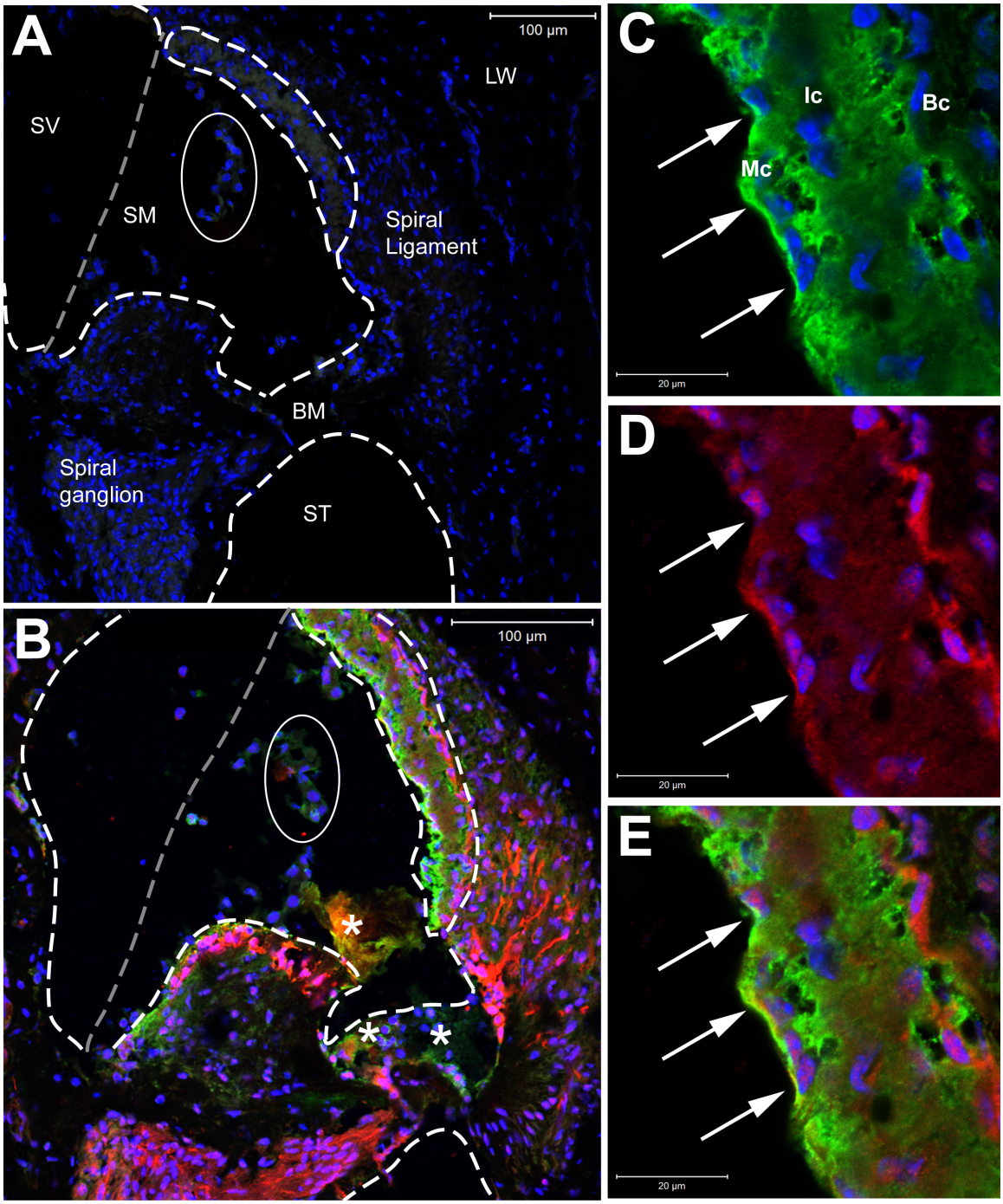
A
100 µm
LW
SV
SM
Spiral
Ligament
BM
Spiral
ganglion
ST
B
100 µm
C
Ic
Bc
Mc
20 µm
D
20 µm
E
20 µm

Figure 18: NKCC1 and NPR-A are occasionally expressed in the same cells within the stria vascularis.
A-B. Scala media sections from CBA 518. A. Control image with no primary antibodies. B. Double-label image of the scala media with anti-NKCC1 (green) and anti-NPR-A (red) with Hoechst (blue). The asterisk indicates labeling in the tectorial membrane and collapsed cells from the organ of Corti. Circle indicates collapsed cells of Reissner's membrane, with the proper location designated with the grey dotted line. C-E. Inserts of the stria vascularis from CBA 518. Arrows indicate areas of co-localization between the two proteins. C. Anti-NKCC1 primary antibody (green). Mc marginal cells. Ic intermediate cells. Bc basal cells. D. Anti-NPR-A primary antibody (red). E. Merged double-label image exhibiting some regions of co-localization (yellow, arrows). Note that the co-localization is infrequent and does not appear as a continuous yellow line throughout the marginal cells. SV Scala vestibuli. SM Scala Media. ST Scala tympani. BM Basilar membrane. LW lateral wall.

Spiral ligament

NKCC1 was found in multiple fibrocytes of the spiral ligament (Fig. 19), most likely within type II[18] and/or IV[38] as these are the closest to the root cell projections[2]. NKCC1 expression extended laterally through fibrocytes of the spiral ligament, but not the root cells. The expression level was less intense in the fibrocytes closer to the stria vascularis (types I, IV, and V[18,68,2]). NKCC1 was not found in root cells of the spiral ligament and consequently was not co-expressed with NPR-A in the spiral ligament.

NPR-A and NKCC1 were intermittently co-localized in some areas of the cochlea, but were separate in other areas (Fig. 20). A sporadic pattern of co-localization was observed in the interdental cells of the spiral limbus and the marginal cells of the stria vascularis. No intercellular localization was noted in the basal cells of the stria vascularis or the cells of the spiral ligament. Furthermore, fibrocytes in the spiral limbus did not exhibit co-localization, but did express both NPR-A and NKCC1. NPR-A and NKCC1 did not co-localize in the spiral ganglion, as NKCC1 expression was not observed in nerve tissue.

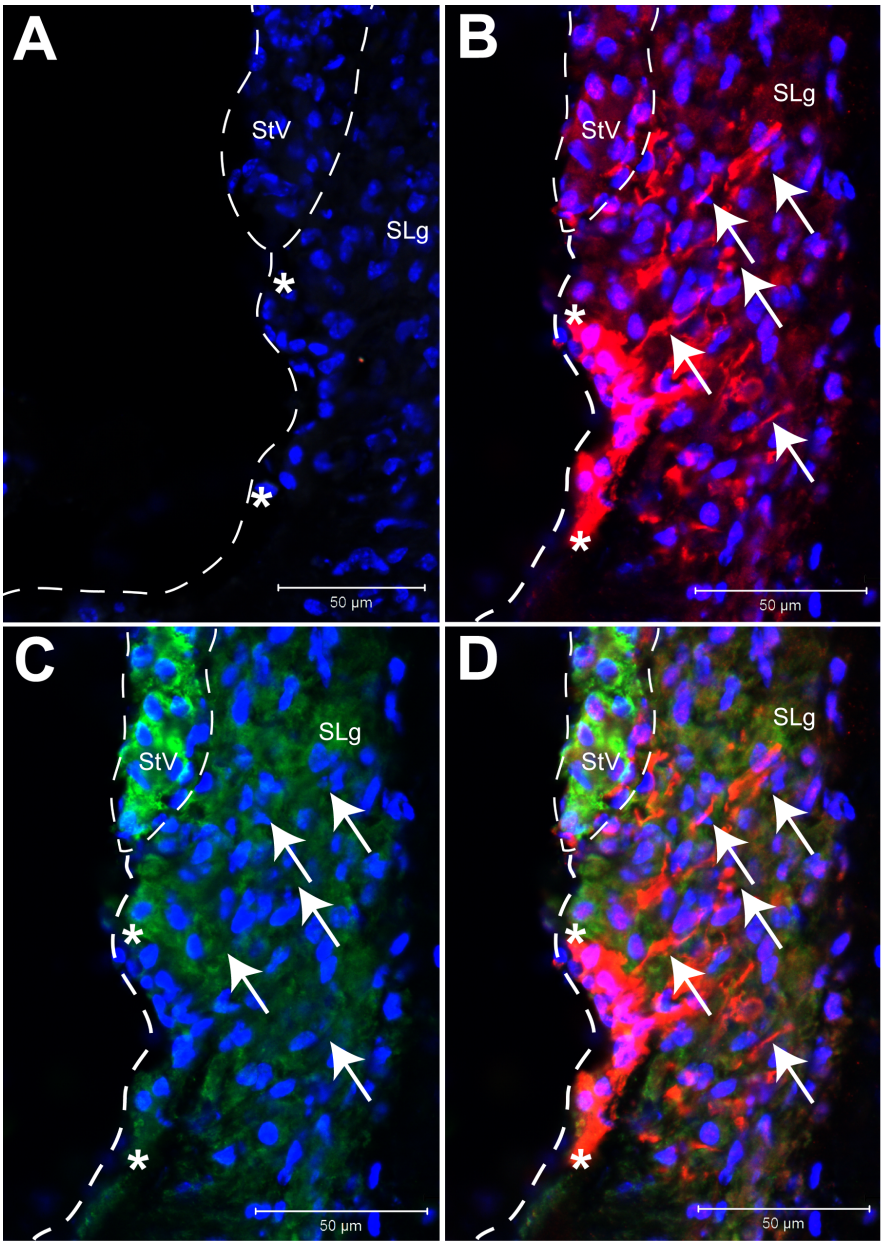

Figure 19: NPR-A and NKCC1 did not co-localize in the spiral ligament.
25x images of the spiral ligament from CBA 596. A. Control section with no primary antibodies. B. Experimental image with anti-NPR-A primary antibody (red). C. Experimental image with anti-NKCC1 (green). D. Merged image showing double label of NPR-A (red) and NKCC1 (green) with Hoechst reagent (blue). Asterisk indicates root cell bodies in the outer sulcus with lateral projections (arrows) or where they would appear (C). Note the lack of overlap between the red NPR-A label of the root cells and the green NKCC1 label of the surrounding fibrocytes. StV stria vascularis. SLg spiral ligament. LW lateral wall.

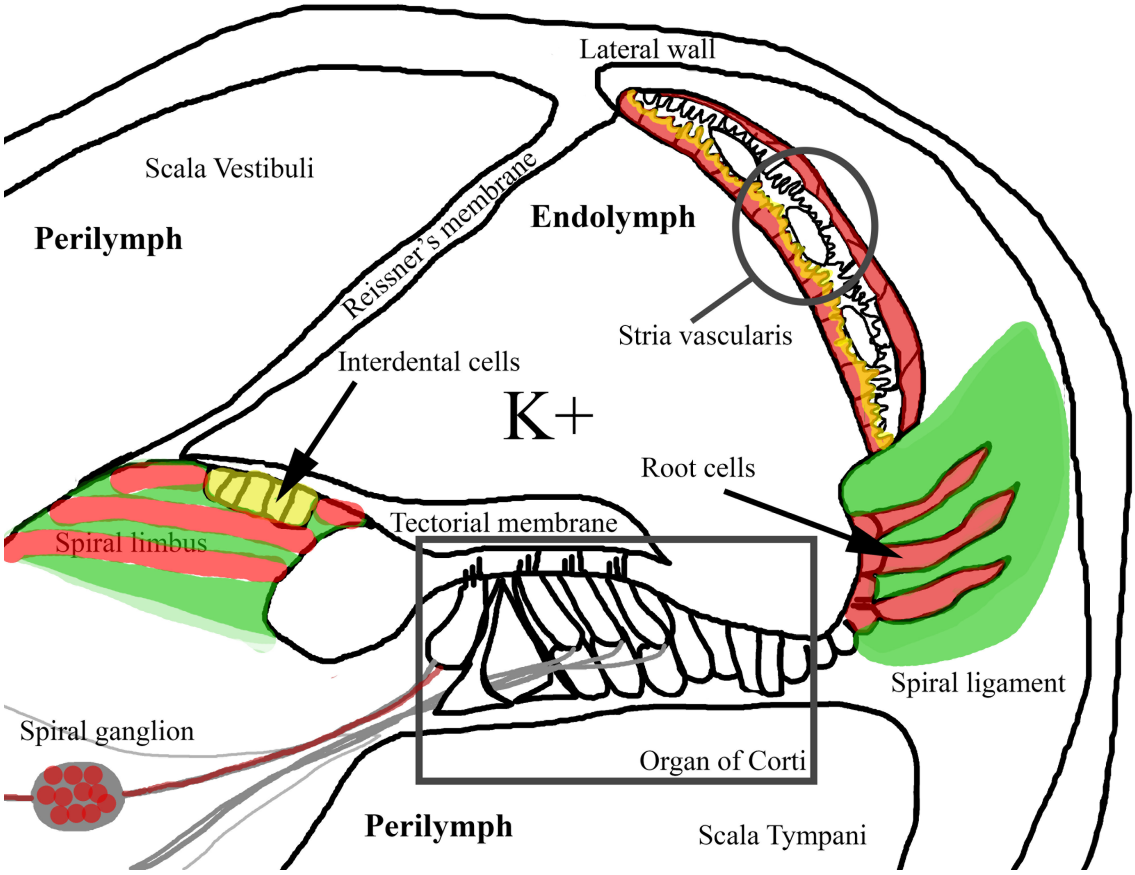

Figure 20: Summary diagram of NPR-A and NKCC1 noting areas of co-localization. Summary diagram of the expression of NPR-A and NKCC1 in the cochlea showing specific regions positive for NPR-A and NKCC1 labeling. Co-localization was the most intense in the interdental cells of the spiral limbus, although still not continuous. Co-localization was also seen in the marginal cells of the stria vascularis. NKCC1 (in fibrocytes) and NPR-A (in root cells) were both expressed in the spiral ligament, but in different cells. NPR-A expression as also seen in the basal cells of the stria vascularis and spiral ganglion cells, where NKCC1 was not found. Some label of both proteins was also observed in the tectorial membrane. For simplicity, areas with co-localization are depicted as solid yellow, however the overlap was intermittent and did not penetrate the entire cell body when observed.

Discussion

NPR-A is acting in two major systems of the cochlea. Firstly, NPR-A is in a position to play a critical regulatory role in the movement of potassium ions through the medial and lateral K^+ recycling systems, based on the labeling pattern of NPR-A in the spiral limbus (Fig. 14 and Fig. 17), the root cells of the spiral ligament (Fig. 14 and Fig. 19), and the basal and marginal cells of the stria vascularis (Fig. 14 and Fig. 15). Secondly, the expression of NPR-A in the cell bodies and central/peripheral processes of the spiral ganglion neurons (Fig. 12 and Fig. 14) indicates that NPR-A may also play a role in neurotransmission within the cochlea. Before discussing the functional implications of these findings, the argument for specificity of label will be presented.

Specificity of Label

The results from control experiments indicated the NPR-A antibodies were performing as expected because 1) the primary antibodies were specific to the antigens (as designed), 2) the secondary antibodies were specific to the primary antibodies, and 3) the positive and negative controls supported the predicted expression patterns in those tissues.

1) Primary antibodies were specific to the antigens

The two antibodies that were used to localize NPR-A targeted different regions of the protein. The N-terminal antibody (Abcam) and the C-terminal antibody (Potter) showed homologous expression patterns of NPR-A in 4 distinct regions of the cochlea with slight variations in expression intensity. Reported data from western blot analyses

was used to assess the quality and specificity of the antibodies, and BLAST searches were performed to determine other potential targets for the antibodies. Also, the staining in the tectorial membrane and organ of Corti will be addressed (label in non-specific tissues).

Using western blot analysis (other labs), the N-terminal (Abcam)[69] and the C-terminal (Potter)[70] antibodies each only yielded one band, suggesting that each antibody only binds to one protein. This information provides evidence that the observed expression pattern in our immunohistochemistry results can be attributed to the NPR-A protein (and not non-specific binding of the antibodies). Experiments using both the N-terminal[69,71–74] and C-terminal[44,56,70] antibodies have been reported, indicating they have been accepted as successful targets for their antigens.

Further support that the primary antibodies were specific to their targets was obtained from BLAST data using the protein databank from the National Center for Biotechnology Information (ncbi.nlm.nih.gov). The search for the antigen targets of the two NPR-A antibodies did not yield the same result i.e. the nearest overlapping protein sequence was not the same for each antibody, making it unlikely that the antibodies were binding to a protein of similar sequence to NPR-A. Iodotyrosine deiodinase had a 45% identity to the NPR-A antigen. Native to the thyroid gland, Iodotyrosine deiodinase (Iyd) is an enzyme that catalyzes deiodination of halogenated byproducts of thyroid hormone production critical to iodide retrieval[75,76], and has not been reported in the inner ear. For the C-terminal antibody (Potter), the closest protein sequence was for asparaginyl endopeptidase (AEP), a lysosomal cysteine protease active on asparagine residues near

C-terminal regions of proteins[77,78], with a 69% protein identity. Important to lysosomal degradation and toll-like receptor maturation, AEP is native to the kidney and spleen and may play a role in red blood cell maturation[77]. Because the BLASTs against the two NPR-A antibodies did not yield the same protein, nor were those proteins (Iyd and AEP) native to the cochlea, it is, therefore, unlikely that the primary antibodies were not binding to other antigens with similar protein sequences.

The N-terminal and C-terminal antibodies had similar expression patterns in the cochlea with two distinct exceptions: intensity of labeling in the stria vascularis and expression pattern of labeled cells in the spiral limbus. The C-terminal target had a lighter intensity of label in both the marginal and basal cells of the stria vascularis (Fig. 14d), but showed identical cellular localization, supporting the conclusion that NPR-A was expressed in these cells of the stria vascularis. The other major difference between the antibodies was the staining in the cells of the spiral limbus, where the N-terminal target was specific only to interdental cells, but the C-terminal target was found in limbal fibrocytes (Fig. 14f).

One explanation for the differences in staining may be the density of the tissue or availability of the antigen, as the C-terminal is internal and may be more difficult to access. A second explanation for both the variations in labeling intensity and the differential expression in limbal fibrocytes is phosphorylation events at the time of tissue collection. As previously mentioned, the C-terminal of the protein is internal to the cell and is near the guanylyl cyclase domain[45,79]. Phosphorylation or dephosphorylation may alter the availability of the C-terminal target. A third explanation for the differences

between the two NPR-A antibodies in the spiral limbus may be glycosylation events in the N-terminal region of the receptor protein. Glycosylation of the N-terminal region (external to the cell, where ANP binds) may affect the affinity of ANP for its receptor[80], suggesting that there may be differing availability of the N-terminal region (the Abcam antibody target) depending on the glycosylation events at the time of tissue collection.

Although unexpected, the expression of NPR-A in the limbal fibrocytes does not change the conclusion that NPR-A is crucial to potassium recycling, as the fibrocytes of the spiral limbus could be a transition point for K^+ from the gap-junction network (see "Role of NPR-A in K^+ recycling" below) to a less differentiated connective tissue gap-junction network in the inner sulcus. This conclusion is further supported by the fact that using the C-terminal (Potter) antibody, we observed NPR-A more heavily on the medial portion of the spiral limbus.

Both NPR-A antibodies and NKCC1 labeled the tectorial membrane, while the Kir4.1 antibody labeled only lightly or not at all in this tissue. The tectorial membrane is a connective tissue secreted by the interdental cells of the spiral limbus[11]. It is composed of three collagen types and three glycoproteins known as tectorins[81,82]. There are several potential explanations for the unexpected labeling of the tectorial membrane by the NPR-A and NKCC1 antibodies. First, these two proteins could secreted by the interdental cells of the spiral limbus as the tectorial membrane is being synthesized. This is purely speculative, however, as there are no reports of transmembrane receptors/channels that can be excreted into the extracellular matrices.

A second, more likely explanation for the observed staining in the tectorial membrane is that the secondary antibodies became "stuck" to the tissue as it is naturally adhesive. There was no label in the control sections (no primary antibody) (Fig. 18a), suggesting that the primary antibody sites did not stick in the tectorial membrane. Additionally, there was no labeling of the tectorial membrane observed with the Kir4.1 antibody, which used the same secondary as the NKCC1 antibody.

Another plausible explanation for labeling in the tectorial membrane may be the blocking agents that were used. NPR-A and NKCC1 both received 1% milk blocking solutions in PB or PBS, while Kir4.1 received amore specific serum blocking solution (Table 4). It is possible the staining in the tectorial membrane was due to the non-specific binding of the NPR-A and NKCC1 secondary antibodies to the milk blocking agent. This possibility would account for the lack of label of Kir4.1 in the tectorial membrane, but does not explain why the secondary antibody bound non-specifically to the tectorial membrane and not other tissues.

Finally, staining in the tectorial membrane may simply be due to the condition of the tissue on the section. During cryosectioning, it was common for tissues like the tectorial membrane and cells in the organ of Corti to fold, creating grooves in the tissue where antibodies could wedge. If this happened, then they may not wash out during labeling. Folding of the tissues was a common problem, as collapsed cells in the organ of Corti, pieces of the cerebellum, and the vestibular system also rarely, but occasionally exhibited un-specific label (Fig. 18b).

2) Secondary antibodies were specific to the primary antibodies

Several experiments were performed to provide more evidence that the observed cochlear labeling was specific to the target proteins. To confirm the observed staining was due to the presence of NPR-A and NKCC1, this study was designed to a) account for background staining, b) use multiple secondary antibody tags, and c) analyze control sections without primary antibodies.

One problem with immunohistochemistry is that there can be too much background staining to observe the specific expression patterns of the antibody. This can be from primary antibodies, secondary antibodies, or both. To avoid this, multiple blocking agents were tested to determine which block provided the least amount of background. Ultimately, the specific blocking solutions were chosen for each antibody based on the level of background expression of antibody dilutions. For example, the N-terminal anti-NPR-A antibody (Abcam) had the least background with a milk/pb block at a 1:50 dilution (Table 4).

A second problem can be non-specific binding of the secondary antibody. To ensure that the observed staining pattern was specific to target protein (and not due to non-specific binding of the secondary antibody), multiple preliminary experiments were performed with secondary antibodies of different hosts and fluorescent ranges (some data not shown). NPR-A was labeled with the Alexa 568 (red) goat anti-rabbit secondary antibody (as observed in the above figures). In separate experiments, NPR-A was labeled using an Alexa 488 (green) donkey anti-rabbit secondary antibody (data not shown). These two secondary antibody labels showed similar expression levels of the NPR-A

protein for the same primary antibody. Based on these preliminary experiments, it is likely that the secondary antibodies were specifically binding to the primary antibodies as designed.

Control sections were run with each experiment using the same protocol, but receiving the blocking agent instead of the primary antibody during the labeling step in order to be sure there was no non-specific binding of the secondary antibodies. Any binding observed in the control sections would be non-specific binding of the secondary antibody. Little to no staining was observed on the control sections, further confirming that the secondary antibodies were specifically binding to the primary antibodies.

During imaging, similar settings were used on the confocal microscope (Table 5) to ensure comparability between the images and experiments. These settings were also conserved between experimental and control (no primary antibody) sections to ensure that background levels were evaluated appropriately. This provided information that the variances in staining intensities observed was not due to different settings upon data collection.

3) Staining Consistent with Previous Reports

In addition to theoretical considerations of binding specificity, the antibody experiments were performed on positive kidney control and negative muscle control tissues where the expression of NPR-A and NKCC1 were already known. These two positive and negative control experiments provide confidence that specific labeling of the NPR-A and NKCC1 protein was observed when expected, and not in tissue that would not express these proteins.

3a) Positive control: staining in the kidney tissue

The kidney was used as a positive control for both NPR-A and NKCC1 as both proteins have both been reported in the kidney using multiple techniques[64,67,83–85]. Using immunohistochemistry, NPR-A has been found in the collecting duct (both medullary[64] and cortical[65]) and in both the renal glomeruli and capillaries[63,84] as observed in this study (Fig. 6). These studies also observed light labeling in the medulla, which can be attributed to either the loop of Henle or the medullary collecting duct[64,84]. It should be noted that there was considerable background labeling of NPR-A in the kidney. While this background label was brighter than the corresponding label in the cochlea, there was more intense specific label in the areas that have been reported to contain NPR-A (Fig. 6 arrows).

NKCC1 has been localized to the glomeruli of the cortex, and the collecting duct in both the cortex and medulla[67,85] as was observed in these experiments. Overall the observed results were consistent with the reported locations, supporting the position that the positive staining observed in the cochlea was specific to the NPR-A and NKCC1 proteins and not due to background staining. The expression patterns of NPR-A and NKCC1 in the kidney indicate the antibodies used in this study were working correctly, as they labeled positive control cells reported to express these proteins, and did not label negative control cells that do not express these proteins.

3b) Negative control: lack of stain in the muscle tissue

In addition, negative control experiments were performed using the quadriceps muscle (Fig. 7). NPR-A[66] and NKCC1[67] have not been reported in skeletal muscle, and

therefore should not be expressed in this tissue. While in the muscle there was a slight color change between the control image and the experimental one, this was most likely due to the natural fluorescence of the tissue or slight background labeling, and less to do with potential positive labeling of the proteins.

3c) LCM and qRTPCR support immunohistochemical results

Using laser capture microdissection to isolate specific cells in concert with qRT-PCR to amplify the NPR-A mRNA and the time of collection should have yielded results about the relative expression levels of NPR-A in specific cells of the cochlea. Ideally, using LCM would provide specific cell isolates from different cochlear regions and thereby provide a basis to quantitatively compare NPR-A mRNA expression between cell populations. Although this experiment was designed as a second confirmation of NPR-A expression in different cochlear regions (in addition to the immunohistochemistry experiments), these data were not entirely successful due to the poor RNA quality and difficulty of performing laser capture microdissection on the cochlea.

While the cochlear LCM extracts did not yield information, important results were captured from the kidney LCM samples and the homogenate tissue samples. These studies were able to confirm the presence of NPR-A mRNA in both kidney and cochlear homogenate samples, concluding that the primers were binding to NPR-A and providing evidence that NPR-A was produced in these tissues. Quantitative PCR demonstrated the presence of NPR-A in the medulla. Usable data were not yielded from the cortex LCM samples, most likely due to the RNA quality and not the fact that NPR-A was not actually present in the kidney cortex. This conclusion is plausible because of the other controls

performed in these experiments to confirm the NPR-A label, as well as support from the literature for NPR-A expression in both the renal medulla and cortex[63,65,84].

While the information about NPR-A expression in these tissues is not novel, the fact that the cochlea, a significantly smaller tissue than the kidney, expressed comparable amounts of NPR-A mRNA as the kidney is significant (Fig. 9). It has long been accepted the NPR-A is a major regulator of the cardiovascular and renal systems, but the effects of NPs on hearing are rarely discussed. Using the qPCR data collected in these studies, NPR-A is likely to have a very significant role in the cochlea due to the expression levels of NPR-A reported. Furthermore, extrapolating from the two LCM samples that showed compatible expression levels to the other tissues, cochlear cells could yield successful mRNA qualitatively similar to the NPR-A expression levels shown in the kidney LCM samples (Fig. 9). The kidney LCM results provide evidence that the NPR-A immunohistochemical labeling is specific to the antigen, and suggests that similar LCM results will be observed in the cochlea.

NPR-A Expression in Cochlear Neurons

NPR-A was detected throughout the entirety of type I spiral ganglion neurons including the central and peripheral processes (Fig. 11 and Fig. 12c). Kir4.1 expression was observed in the Schwann cells of the spiral ganglion, but not the cell bodies of the neurons (data not shown). Co-localization between NPR-A and Kir4.1 was not observed in these cells, suggesting NPR-A was found only in the neurons themselves. There is no definitive molecular marker to distinguish between type I and type II spiral ganglion cells, but there are several lines of evidence that NPR-A was expressed in only type I

spiral ganglion cells for three main reasons. Firstly, the cell bodies that stain with NPR-A were located throughout the spiral ganglion and not just on the periphery. Secondly, the morphology of the cell bodies coincided with descriptions of Type I spiral ganglion cells in that they were large, spherical bodies. Lastly, NPR-A expression was clearly in the peripheral processes of the spiral ganglion that communicate with inner hair cells (Type I) (Fig. 11), but not within the basilar membrane or underneath the outer hair cells, which would indicate expression in Type II neurons. Taken together, these results support attribution of NPR-A to type I spiral ganglion neurons, but not type II neurons. This novel finding may indicate NPR-A could be used as a molecular marker to distinguish between spiral ganglion neurons. Further experiments need to be performed in order to explicitly confirm NPR-A expression was localized to only type I spiral ganglion neurons.

While the evidence indicates that NPR-A was expressed in spiral ganglion cells, these cells are not components of the K^+ recycling system and therefore the presented hypothesis would not have predicted the expression of NPR-A in that region. Nevertheless, there are several potential functions for NPR-A in spiral ganglion neurons.

There is recent evidence that NPs may function in a number of roles in the central nervous system including neural development, neurotransmitter uptake and release, regulation of synaptic function, and/or neuroprotection[86]. While NPR-A may not be in the spiral ganglion because of the K^+ gateway, it may have functional roles other than ion transport in the cochlea. NPR-A has been localized to the trigeminal nerve, where activation by BNP may play a role in nociception and as a delayed regulator to sensory

excitability[72]. These authors suggested that BNP/NPR-A secondary messenger activation might have antinociceptive functions in the trigeminal nerve. NPR-A has also been localized to the dorsal root ganglion. Activation of NPR-A by BNP may play a role in scratch response and itch detection[74].

In the brain, NPR-A mRNA expression has been localized to the subfornical organ and habenula of the central nervous system[86]. The subfornical organ plays a role in osmoregulation[87] as well as regulation of the cardiovascular system[87,88]; NPs are known regulators of these two systems. The habenula has functional roles in pain processing, sleep-wake cycles, mood and depression, nutrition, stress response, and learning[89]. Although the presence of NPR-A in the spiral ganglion was not anticipated, NPs and in turn their receptors have been localized to the nervous system. Therefore, NPR-A may have a functional role in signal processing of spiral ganglion neurons.

NPR-A expression in gateways for K^+ recycling

NPR-A was found in areas of transition in the K^+ recycling systems i.e. regions where K^+ must flow between different cell types or exit into the endolymph. As previously described, the movement of potassium ions in the cochlea is highly regulated and critical to hearing. K^+ cycles through the cochlea in two major directions: 1) in the outer sulcus system from the outer hair cells laterally through the spiral ligament and out of the stria vascularis into the scala media (Figs. 1 and 21 blue)[2] and 2) in the inner sulcus system from the inner hair cells medially through the spiral limbus and out of the interdental cells into the scala media (Figs. 1 and 21 purple)[11]. Based on the expression

of NPR-A in the spiral limbus, spiral ligament, and the stria vascularis, NPR-A was clearly localized to cells that are vital to the transition of K^+ these two systems.

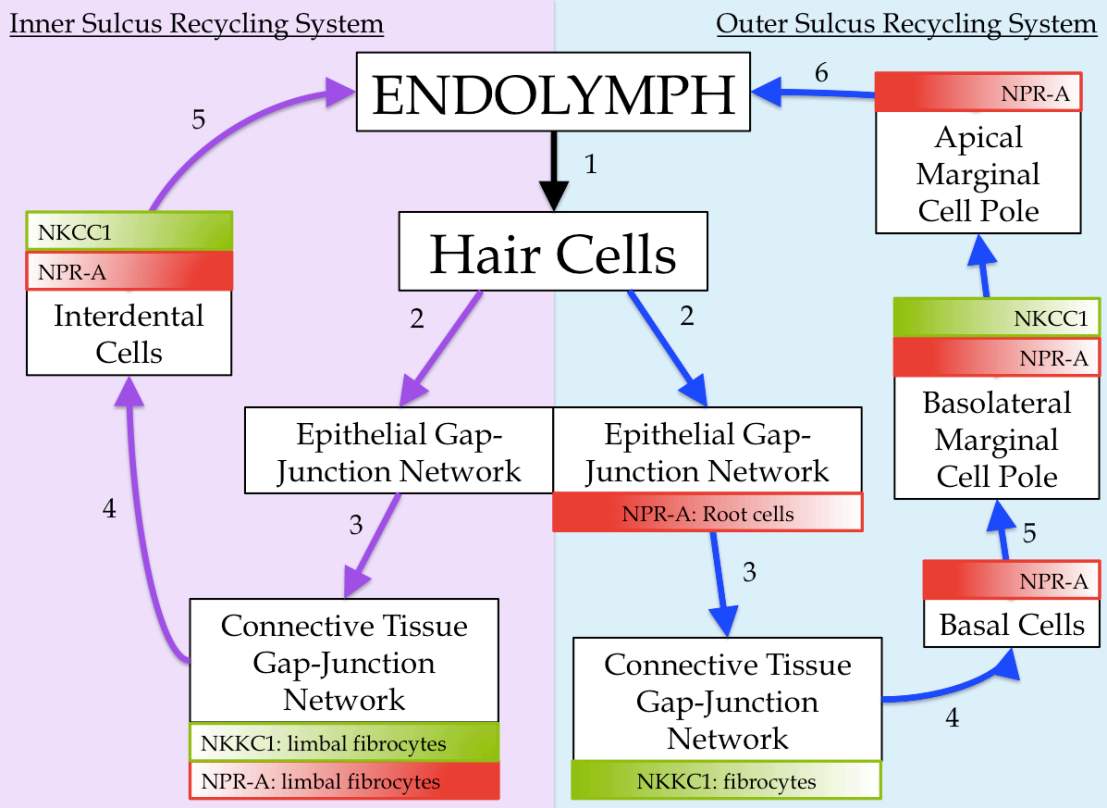

Figure 21: NPR-A and NKCC1 Expression in gateways for K+ transition in the inner and outer recycling systems.
NPR-A is expressed in cells key for K^+ movement either into or out of different cellular networks, or from a cell into the endolymph. This expression pattern implicates NPR-A as a key regulator for K^+ transition from the different recycling networks. The numbers indicate the gateway for K^+ movement with the inner sulcus system has 5 gateway points and the outer sulcus system has 6 gateways. There is no number between the basolateral and apical marginal cell boxes as they are within the same cell where K^+ can freely diffuse.

1) NPR-A expression in the outer sulcus K^+ recycling system

There are six gateways where the movement of K^+ can be regulated in the outer sulcus system: 1) into the apical pole of the outer hair cells via the mechanotransduction channels, 2) between the outer hair cell basal pole and the epithelial gap-junction network

of the organ of Corti, 3) between the root cells in the outer sulcus and the fibrocytes of the connective tissue gap-junction network in the spiral ligament, 4) between the connective tissue gap-junction network and the basal cells of the stria vascularis, 5) from the intrastrial space into the basolateral pole of the marginal cells, and 6) from the luminal surface of the marginal cells of the stria vascularis into the endolymph. Within the outer sulcus system, NPR-A was expressed in four of these six transition points (Fig. 21 blue panel). This evidence suggests a critical regulatory role for ANP in the movement of K^+ through transitioning systems/cell types.

NPR-A was not expressed in the outer hair cells or any of the supporting cells of the organ of Corti. Therefore, it is unlikely NPR-A plays a regulatory role in K^+ movement through the first two gateways of the outer sulcus recycling system (1- into the apical pole of the outer hair cells and 2- exit from the basolateral pole of the hair cells into the epithelial gap-junction network). In these areas, K^+ travels out of the basolateral pole of the outer hair cells via Kv7.4[35,90] and into Dieter's cells via KCC3 and KCC4 and to some degree Kir4.1[2,36]. There are no reports that NPR-A activates any of these transporters or channels in other tissues.

NPR-A expression in the root cell gateway

NPR-A was heavily expressed in the third gateway for K^+ transition in the outer sulcus K^+ recycling system: the root cells of the spiral ligament (Fig. 19). Functionally, root cells are the part of the epithelial gap-junction network[2,91] and represent the transition point where K^+ ions must move out of the epithelial gap-junction network into the connective tissue gap-junction network[2]. NKCC1 was also expressed in the spiral

ligament but specifically not in the root cells and therefore, the downstream effector for NPR-A in the root cells is unknown.

NPR-A expression in the basal cell gateway

Once K^+ transitions into the connective tissue gap-junction network (third gateway Fig. 21 blue side), it can flow between fibrocytes of the spiral ligament and into the stria vascularis (fourth gateway Fig. 21 blue side). NPR-A was heavily expressed in the basal portion of the basal cells of the stria vascularis in the region where K^+ flows from ligamental fibrocytes into the basal cells via gap-junctions. There are conflicting opinions of which fibrocytes form gap-junctions with the basal cells. Spicer and Schulte (1996) propose type Ia and Ib fibrocytes connect with the basal cells[18], while Zdebik *et al.* (2009) claim it is types IV and V[3].

Although basal cells are connected to the fibrocytes via gap-junctions[3,20,26], the nature of the K^+ gradient would suggest it would be optimal to have regulation of the gap-junctions to ensure K^+ movement into the high voltage/low K^+ concentration internal environment in the intrastrial space. Although there are no reports of cGMP regulation of gap-junctions, there is evidence that the assembly of and communication through gap-junctions can be affected by second messengers like cAMP[92,93]. Furthermore, cAMP reduces the permeability of Connexin-26[94], a major component of most cochlear gap-junctions[95], likely acting to control the flow of K^+ into the basal cells. Although this gateway for K^+ exhibits less physical segregation than in root cells [i.e. there are gap-junctions rather than separated cells between the two systems], NPR-A may still act as a regulator for K^+ by modifying traffic through the gap-junctions, and thereby controlling

K^+ influx from the connective tissue gap-junction to the stria vascularis. Therefore, the natriuretic peptide cascade triggered by NPR-A activation may also influence passive K^+ transport through pores and not just active K^+ transport.

NPR-A expression in the marginal cell gateway

Marginal cells account for the final two gateways for K^+ recycling through the outer sulcus system. Potassium ions travel into the marginal cells basolaterally from the intrastrial space (gateway 5). K^+ is then excreted into the endolymph along the apical portion of the marginal cells via KCNQ1 (gateway 6) (Fig. 21). NPR-A was expressed throughout the entire marginal cell (Fig. 18), implying that the secondary messenger cascade may stimulate transporters for both K^+ influx and efflux within the marginal cells.

The intrastrial space lateral to the marginal cells has an extremely high voltage (100 mV), but low K^+ concentration (Fig. 2). K^+ is moved from the basal cells to the intermediate cells via gap-junctions (Connexins 26 and 30)[3]. Once in the intermediate cells, Kir4.1 leaks K^+ into the intrastrial space creating the endocochlear potential. The marginal cells take up K^+ basolaterally through several transporters including NKCC1 and Na^+/K^+ ATPase[23,26]. K^+ moves out of the stria vascularis on the luminal surface of the marginal cells[26], thus completing the K^+ recycling pathway of the outer sulcus system.

NPR-A mRNA has been found in the stria vascularis using whole strial cell isolation and PCR[52]. However, this work did not distinguish among the different cell types composing the stria vascularis. Qiao *et al.* showed NPR-A and ANP expression via

RTPCR in cultured marginal cells isolated from the stria vascularis [53]. Consistent with these findings, in this study, both the N-terminal and C-terminal anti-NPR-A antibodies localized NPR-A expression to the marginal cells.

Co-localization between NPR-A and Kir4.1 was not observed (Fig. 15), suggesting any NPR-A label in the intermediate layer of the StV was due to marginal cell projections that penetrate the layers of the StV to the basal cell layer (Fig. 2). Some of this expression could be due to the basal cell projections, however they do not penetrate the intermediate cell layer as deeply as marginal cells[20]. Furthermore, while Kir4.1 is commonly used as a marker for intermediate cells[96], it is possible co-localization was not observed as the label may not penetrate the entire cell body. However, the lack of any co-localization between NPR-A and Kir4.1 indicates NPR-A was likely only expressed in the marginal and basal cells of the stria vascularis.

NPR-A was expressed throughout the body of the marginal cells and intermittently co-expressed with NKCC1, which was local only to the basolateral plasmalemma (Figs. 18 and 20). Because NPR-A was expressed throughout the whole marginal cell, and not just one pole, it could regulate both K^+ influx basolaterally via NKCC1 and K^+ efflux apically through an unknown effector. This is an important finding in that movement of K^+ is critical to maintain proper hearing function. Research in the cardiovascular system and ovary has shown there is a functional phenotypic link between gene mutations in *KCNQ1* and *NPPA* (natriuretic peptide precursor A), a gene that codes for ANP (the ligand of NPR-A). Using a registry of patients with familial atrial fibrillation, 231 people expressed both of the mutations and exhibited symptoms of

early onset lone atrial fibrillation. These results suggest two different mutations in the 4q25 chromosomal loci lead to the same phenotypic condition[97,98]. This information may imply there is also a functional connection between KNCQ1 and NPs in the inner ear, which reflects many of the same protein relationships the cardiovascular and renal systems express in regards to NPs and their effectors.

2) NPR-A expression in the inner sulcus K^+ recycling system

There are five gateways for K^+ transition in the inner sulcus system: 1) into the inner hair cells from the endolymph via the mechanotransducer channel, 2) out of the inner hair cells and into the medial epithelial gap-junction network, 3) through the epithelial gap-junction network and into the limbal fibrocytes, 4) from the limbal fibrocytes into the interdental cells, and 5) out of the interdental cells to the endolymph. While the movement of K^+ through the outer sulcus system has been well documented, the movement through the inner sulcus recycling system is much less understood. In the inner sulcus recycling system, there are fewer gateways and less functional segregation between cells. Anatomically, there is a less clear transition between inner sulcus cells and limbal fibrocytes. This medial system is more analogous to the flow of K^+ in the vestibular system, where there is less development of specific cell types and segregation of networks[11].

In a similar manner to the outer sulcus recycling system, NPR-A was not expressed in the first two gateways of the inner sulcus recycling system (1- influx through the MET channel into the apical pole of the inner hair cells and 2- efflux from the inner hair cells in to the underlying supporting epithelial gap-junction network). As

in the outer hair cells, K^+ exits the inner hair cells via multiple K^+ channels and to a lesser degree, Kir7.4[90], and is then taken up by inner phalangeal cells of the organ of Corti via KCC3[3,36]. Inner phalangeal cells do not express KCC4[3,36].

NPR-A Expression in the limbal fibrocytes

Using the C-terminal antibody (Abcam), NPR-A was identified in the limbal fibrocyte network of the spiral limbus (third gateway) (Fig. 14), where K^+ exits the epithelial gap-junction system and enters the spiral limbal fibrocytes. There is little information about what makes a cell a limbal fibrocyte versus an inner sulcus cell, so there may be some overlap between these regions[11]. Functionally, this area is likely analogous to the root cell gateway in the outer sulcus recycling system, although it is unclear whether this pathway delineated as the pathway via the root cells. Using the C-terminal antibody (Potter), NPR-A was expressed along the inner sulcus and therefore may act to influence an effector in this region. Furthermore, NPR-A may act medially through fibrocytes on the other side of the spiral limbus and consequently regulate flow in this region. Even though the inner sulcus recycling system is not as distinguished as the outer sulcus system, NPR-A was still positioned in areas critical for K^+ transition between networks or cells.

NPR-A Expression in the interdental cell gateways

NPR-A was localized to the fourth gateways involving the interdental cells in a manner similar to the marginal cells of the outer sulcus recycling system. Based on the current anatomical knowledge about this tissue, it is unclear if there are two separate gateways (analogous to the stria vascularis in the outer sulcus system), or if there is only

one transition point. Interdental cells act to sequester compounds from the limbal fibrocytes and export them into the endolymph[12,18]. Therefore, activation of NPR-A in these cells may cause stimulation of transporters to move K^+ into the cell along the basolateral pole and/or out of the cell apically via KCNQ1 (similar to marginal cells in the stria vascularis).

Comparison with previous localization studies

Reports describing the presence of NPR-A in the cochlea provide inconsistent descriptions regarding the precise localization to specific cell types, which necessitated the design of this study. Most previous reports agree that NPR-A is localized to the lateral wall, but there are differing opinions of which cells specifically express NPR-A. NPR-A was first found in the cochlea in studies that used audioradiography, which showed that it was present in the stria vascularis, but not the organ of Corti[42,51,99]. Using *in situ* hybridization, NPR-A was found in the spiral ligament and the Schwann cells of the cochlear nerve, but not the stria vascularis[41,54]. The results presented in this manuscript support the audioradiography and *in situ* hybridization data that NPR-A was present in the StV and spiral ligament. By contrast, in this study NPR-A was localized to the spiral ganglion neurons and not the Schwann cells (Fig. 11 and Fig. 16). PCR of strial mRNA showed expression of NPR-A in the stria vascularis, but did not provide information about expression within individual cell types[52]. Furthermore, NPR-A mRNA has been found in cultured marginal cells, but this study was not able to provide detailed information about positional expression in the intact organ[53]. The current experiments using immunohistochemistry and qRT-PCR provide novel information not only about the

specific tissue expression of NPR-A, but also its morphological relationship to two other proteins expressed in the cochlea (NKCC1 and Kir4.1). This work provides critical information about the potential role of NPR-A in K^+ recycling and neurotransmission, and further supports the hypothesis that natriuretic peptides play important roles in hearing.

Natriuretic Peptide System in the Cochlea

The combination of NPR-A expression in the interdental cells of the spiral limbus, the root cells of the spiral ligament, and the basal and marginal cells of the stria vascularis supports the hypothesis that NPR-A is expressed in areas critical for K^+ movement. More specifically, these five cell types [root cells, basal cells, marginal cells, limbal fibrocytes, and interdental cells] are all in gateway areas where K^+ is transitioning from either a tissue type/specific network or out of a tissue and into the endolymph. This novel information addresses questions with respect to the role(s) NPR-A is playing within the cochlea. Binding of atrial natriuretic peptide presumably leads to activation of NPR-A in these areas, jumpstarting the recycling of K^+ and contributing to the maintenance of hearing thresholds. These interpretations are supported by evidence that NPR-A knockout mice exhibit progressive high-frequency hearing loss[50], which cannot be reversed by infusion of ANP[49]. Data were also obtained in this study that provide information regarding the mechanism underlying the actions of ANP in the cochlea. Two aspects of the ANP/NPR-A pathway will be discussed below: 1) ANP/NPR-A interaction and 2) potential downstream effectors for NPR-A.

1) ANP/NPR-A Interaction in the Cochlea

The first step in the ANP pathway is the binding of ANP to NPR-A causing the generation of cGMP from GTP. ANP can be delivered systemically to the inner ear via the blood vessels of the stria vascularis[49], which represents signaling in an endocrine fashion. With ANP delivery specific only to cells near the blood supply, it could be hypothesized that NPR-A expression would be localized in and around only cells where ANP is systemically delivered (strial vascular cells). However, this hypothesis was not reflected in the results of this experiment, as NPR-A was expressed in 6 cells types in 4 different regions of the cochlea, and not just in cells of the blood vessels of the stria vascularis. Although the mechanism for systemic ANP activation of NPR-A in the cochlea remains undetermined, ANP could also act in a paracrine or autocrine fashion. There is evidence that ANP can be produced in the cochlea, as the activating hormone, corin, has been localized within the stria vascularis, organ of Corti, and modiolus of the inner ear using RT-PCR[100]. If ANP is produced in the cochlea, it is conceivable that NPR-A would be expressed in tissues not directly in diffusion range of the blood supply from the stria vascularis. This hypothesis was reflected in the results of this experiment, with NPR-A expression in six cell types that are physically separated from cochlear blood vessels.

Looking at the pathway of activation, ANP (or BNP) binds to NPR-A triggering events in the kinase homology domain (Fig. 4) [dephosphorylation[45,66], phosphorylation[62,83,101], or both]. This action causes a conformational change in the internal pole of the receptor, dimerizing the guanylyl cyclase domain leading to the

generation of cGMP[66]. Natriuretic peptides affect this system, as systemic delivery of ANP causes a marked increase in the production of cGMP in the cochlea[102]. This second messenger system then acts to stimulate other molecular activators such as PKG. Ultimately, the activation of NPR-A by ANP leads to a change in hearing, presumably due to effectors in the proposed ANP pathway to change the endocochlear potential.

2) Potential Effectors for NPR-A in the Cochlea

Once NPR-A has activated PKG, it can theoretically influence the activity of a number of different channels and transporters causing the observed change in hearing thresholds. While the beginning of the pathway has been determined by the work on natriuretic peptides in our lab[49,50], other labs[41,42,51,53,99], and other systems[40,79,103], little work is being done to connect the natriuretic peptide system to the downstream effectors that could result in changes to auditory thresholds. The results of this study provide a direct link to what is known about cochlear function and what is known about the role of natriuretic peptides in fluid and ion regulation.

Looking at the relationship between NPR-A and NKCC1, it was clearly a more complicated answer than, "yes NKCC1 is the only effector for NPR-A" or "NPR-A is the only regulator of NKCC1". In the six cell types that showed NPR-A expression, a) two cell types may intermittently use NKCC1 as an effector (marginal cells and interdental cells) as some co-localization was observed, and b) four cell types did not show co-expression of NPR-A and NKCC1 (basal cells, root cells, limbal fibrocytes, and spiral ganglion did not express NKCC1) and therefore must use another effector. There is a possibility that cGMP could diffuse between cells expressing NPR-A and then activate

proteins in adjacent cells containing NKCC1 meaning there is a possibility NKCC1 could still be an effector in the ANP pathway when co-localization is not observed. It should also be noted that the discussions below are based on the observed co-localization patterns alone and not on any functional studies.

2a) Cells that might use NKCC1 as an effector

NPR-A in marginal and interdental cells occasionally co-localized with NKCC1, implicating this transporter as an effector activated by ANP. Marginal cells are the major output source for K^+ from the intrastrial space where intermediate cells generate the endocochlear potential. A critical channel is KCNQ1, which is present along the luminal surface of the marginal cells[90,104,105]. Based on the degree of co-localization between NPR-A and NKCC1 in the interdental and marginal cells was intermittent, NKCC1 may not be the only protein important to K^+ movement that is stimulated by the activation of NPR-A in these areas.

Looking specifically at marginal cells, it is interesting to consider the expression of NPR-A appears throughout the entire cell body and not just one pole. In turn, it can be inferred that NPR-A may be important in activating proteins responsible for both K^+ influx in one pole and other proteins responsible for K^+ efflux on another pole. In the marginal cells, intake is attributed to Na^+/K^+ ATPase and NKCC1 basolaterally, and export to the endolymph is from KCNQ1 expressed along the luminal surface[104]. Furthermore, for both cell types NKCC1 was clearly not the only effector (as co-localization was sporadic), and therefore it could also stimulate export proteins for K+ efflux into the endolymph, such as KCNQ1. While the physical relationship of NPR-A to

KCNQ1 is not known, ANP has been documented to influence the expression level of KCNQ1 in cancer cells[106]. In interdental cells, it is unclear if a similar situation occurs with the distribution of transporters (NKCC1 for K^+ influx and another transporter activated for K^+ export).

2b) Cells that do not use NKCC1 as an effector

NKCC1 expression was not observed in the spiral ganglion, indicating these cells have to be utilizing another effector protein in the ANP pathway. NPR-A expression in neuronal tissue is a relatively new observation[72,74,86], and is therefore still being determined. In both strial basal cells and the root cells of the spiral ligament, NKCC1 was localized to the region, but did not co-localize with the cells expressing NPR-A. Because the expression of NKCC1 and NPR-A in these regions were so segregated, the relationship between the two was clear, in that stimulation of K^+ movement by NPR-A must be attributed to another protein or by diffusion of cGMP (or another messenger) across cell membranes. Therefore it is unlikely NKCC1 becomes stimulated by the activation of NPR-A in root cells and basal cells. Although it is unlikely that NKCC1 is the only effector in the ANP pathway, it is possible the secondary messengers may move between cells to stimulate the effector instead of along the same membrane.

There are many other protein targets that could function as effectors following activation of NPR-A in the cochlear ANP pathway. For cells in the spiral ligament, this could be an aquaporin or a potassium channel. Zdebik *et al.* propose the movement of potassium ions into the fibrocytes is due to efflux by KCC3 in the root cells and uptake by Na^+/K^+ATPase in type III fibrocytes[3]. For basal cells, NPR-A might influences the

connexins of the gap-junction networks to regulate the flow of K^+ influx into the stria vascularis[107].

Another potential effector in the ANP pathway is aquaporin 6 (AQP6). Aquaporins are transmembrane channels responsible for the movement of water ions. AQP6 is a significant component of the kidney epithelium[108,109]. Specifically, AQP6 is the only aquaporin found in renal podocytes (a region that expresses NPR-A), suggesting its potential role in glomerular filtration[109]. In the inner ear, AQP6 expression has been shown in the interdental cells of the spiral limbus[109] and along the luminal surface of the marginal cells in the stria vascularis[110], both areas that express NPR-A.

Conclusions

These studies were designed to answer two main hypotheses: (1) NPR-A expression in the cochlea is in areas critical to fluid balance and K^+ recycling and (2) NPR-A expression is co-localized to an effector protein, NKCC1, essential for K^+ movement. The first hypothesis was supported, while the second hypothesis was only partially supported, as co-localization with NKCC1 was intermittent or not present. In the cochlea, NPR-A expression was observed in six specific cell types: interdental cells and limbal fibrocytes of the spiral limbus, root cells of the spiral ligament, basal and marginal cells of the stria vascularis, and spiral ganglion neurons. NPR-A was clearly expressed in cells critical for the movement of K^+, as these cells act as a gateway point for K^+ efflux from a cellular system or influx into a cellular network. NPR-A was expressed in two cell types (marginal cells of the stria vascularis and interdental cells of the spiral limbus) where K^+ must exit a cellular network and re-enter the endolymph[35].

Both conclusions indicate an essential role for the ANP pathway in the regulation of K^+ transition during recycling.

NPR-A was also expressed in type I spiral ganglion neurons, cells critical to carrying the sensory input stimulated by the inner hair cells. While this finding was unexpected, NPR-A has been localized to other neurons important for functions such as nociception[72] and itch response[74] indicating a common importance of NPR-A in the regulation of sensory functions.

The second hypothesis that NPR-A co-localizes with NKCC1 implicating the protein as a downstream effector in the ANP pathway was less definitively proven. In both marginal cells and interdental cells, NKCC1 is a likely downstream target for NPR-A because of the observed intermittent co-localization. In these cells NPR-A could be acting both for K^+ influx into the cells and K^+ efflux into the endolymph, indicating the ANP cascade likely stimulates multiple effectors. Unless cGMP diffuses between cells, clearly another effector must be activated in other cochlear cell types, as co-localization was not observed. These areas include the spiral ligament root cells and fibrocytes and the basal cells of the stria vascularis. In these two areas, NKCC1 was present in nearby cells, but did not co-localize with NPR-A indicating a need for another effector protein in the ANP cascade.

In summary, NKCC1 does not appear to be the main effector stimulated by NPR-A activation in the cochlea, as co-localization within individual cells was infrequent. However, there are numerous potassium channels, aquaporins, and other transporters in the cells of the cochlea that may act as potential downstream targets for NPR-A

secondary messengers. NPR-A was expressed in cells acting as a gateway for K^+ potentially signifying a critical role in K^+ recycling and implicating other effectors in this pathway. Furthermore due to the observed expression profiles, NPR-A likely stimulates transporters/channels for both influx and efflux of K^+ from cells. While future studies need to be performed to identify the proteins comprising the components of the ANP pathway, the results of this study provide novel information about where ANP may act in the cochlea.

Bibliography

1. Potter, L. R. Natriuretic Peptides, Their Receptors, and Cyclic Guanosine Monophosphate-Dependent Signaling Functions. *Endocr. Rev.* 27, 47–72 (2005).
2. Hibino, H. & Kurachi, Y. Molecular and Physiological Bases of the K+ Circulation in the Mammalian Inner Ear. *Physiology* 21, 336–345 (2006).
3. Zdebik, A. A., Wangemann, P. & Jentsch, T. J. Potassium ion movement in the inner ear: insights from genetic disease and mouse models. *Physiol. Bethesda Md* 24, 307–316 (2009).
4. Békésy, G. v. DC Potentials and Energy Balance of the Cochlear Partition. *J. Acoust. Soc. Am.* 23, 576–582 (1951).
5. Kawashima, Y. *et al.* Mechanotransduction in mouse inner ear hair cells requires transmembrane channel-like genes. *J. Clin. Invest.* 121, 4796–4809 (2011).
6. Pan, B. *et al.* TMC1 and TMC2 Are Components of the Mechanotransduction Channel in Hair Cells of the Mammalian Inner Ear. *Neuron* 79, 504–515 (2013).
7. Platzer, J. *et al.* Congenital Deafness and Sinoatrial Node Dysfunction in Mice Lacking Class D L-Type Ca2+ Channels. *Cell* 102, 89–97 (2000).
8. Catterall, W. A. Voltage-Gated Calcium Channels. *Cold Spring Harb. Perspect. Biol.* 3, a003947 (2011).
9. Salt, A. N., Melichar, I. & Thalmann, R. Mechanisms of endocochlear potential generation by stria vascularis. *The Laryngoscope* 97, 984–991 (1987).
10. Marcus, D. C., Wu, T., Wangemann, P. & Kofuji, P. KCNJ10 (Kir4.1) potassium channel knockout abolishes endocochlear potential. *Am. J. Physiol. Cell Physiol.* 282, C403–407 (2002).
11. Spicer, S. S. & Schulte, B. A. Evidence for a medial K+ recycling pathway from inner hair cells. *Hear. Res.* 118, 1–12 (1998).
12. Von Ilberg, C. [Electron microscopic studies on the diffusion and resorption of thorium dioxide in the cochlea of the guinea pig. 3. Limbus spiralis]. *Arch. Für Klin. Exp. Ohren- Nasen- Kehlkopfheilkd.* 192, 163–175 (1968).
13. Barclay, M., Ryan, A. F. & Housley, G. D. Type I vs type II spiral ganglion neurons exhibit differential survival and neuritogenesis during cochlear development. *Neural Develop.* 6, 33 (2011).
14. Brown, M. C., Berglund, A. M., Kiang, N. Y. & Ryugo, D. K. Central trajectories of type II spiral ganglion neurons. *J. Comp. Neurol.* 278, 581–590 (1988).
15. Spoendlin, H. Anatomy of cochlear innervation. *Am. J. Otolaryngol.* 6, 453–467 (1985).
16. Eybalin, M. Neurotransmitters and neuromodulators of the mammalian cochlea. *Physiol. Rev.* 73, 309–373 (1993).
17. Dallos, P. Cochlear amplification, outer hair cells and prestin. *Curr. Opin. Neurobiol.* 18, 370–376 (2008).
18. Spicer, S. S. & Schulte, B. A. The fine structure of spiral ligament cells relates to ion return to the stria and varies with place-frequency. *Hear. Res.* 100, 80–100 (1996).

19. Jagger, D. J., Nevill, G. & Forge, A. The Membrane Properties of Cochlear Root Cells are Consistent with Roles in Potassium Recirculation and Spatial Buffering. *JARO J. Assoc. Res. Otolaryngol.* 11, 435–448 (2010).
20. Spicer, S. S. & Schulte, B. A. Novel structures in marginal and intermediate cells presumably relate to functions of apical versus basal strial strata. *Hear. Res.* 200, 87–101 (2005).
21. Forge, A. The endolymphatic surface of the stria vascularis in the guinea-pig and the effects of ethacrynic acid as shown by scanning electron microscopy. *Clin. Otolaryngol.* 5, 87–95 (1980).
22. SMITH, C. A. Structure of the stria vascularis and the spiral prominence. *Ann. Otol. Rhinol. Laryngol.* 66, 521–536 (1957).
23. Crouch, J. J., Sakaguchi, N., Lytle, C. & Schulte, B. A. Immunohistochemical localization of the Na-K-Cl co-transporter (NKCC1) in the gerbil inner ear. *J. Histochem. Cytochem. Off. J. Histochem. Soc.* 45, 773–778 (1997).
24. Delpire, E., Lu, J., England, R., Dull, C. & Thorne, T. Deafness and imbalance associated with inactivation of the secretory Na-K-2Cl co-transporter. *Nat. Genet.* 22, 192–195 (1999).
25. Eckhard, A. *et al.* Co-localisation of Kir4.1 and AQP4 in rat and human cochleae reveals a gap in water channel expression at the transduction sites of endocochlear K+ recycling routes. *Cell Tissue Res.* 350, 27–43 (2012).
26. Wangemann, P. Supporting sensory transduction: cochlear fluid homeostasis and the endocochlear potential. *J. Physiol.* 576, 11–21 (2006).
27. Takeuchi, S., Ando, M. & Kakigi, A. Mechanism generating endocochlear potential: role played by intermediate cells in stria vascularis. *Biophys. J.* 79, 2572–2582 (2000).
28. Carlisle, L., Steel, K. & Forge, A. Endocochlear potential generation is associated with intercellular communication in the stria vascularis: structural analysis in the viable dominant spotting mouse mutant. *Cell Tissue Res.* 262, 329–337 (1990).
29. Ando, M., Edamatsu, M., Fukuizumi, S. & Takeuchi, S. Cellular localization of facilitated glucose transporter 1 (GLUT-1) in the cochlear stria vascularis: its possible contribution to the transcellular glucose pathway. *Cell Tissue Res.* 331, 763–769 (2008).
30. Hinojosa, R. & Rodriguez-Echandia, E. L. The fine structure of the stria vascularis of the cat inner ear. *Am. J. Anat.* 118, 631–663 (1966).
31. Echandia, E. L. R. & Burgos, M. H. The fine structure of the stria vascularis of the guinea-pig inner ear. *Z. Für Zellforsch. Mikrosk. Anat.* 67, 600–619 (1965).
32. Kimura, R. S. & Schuknecht, H. F. The Ultrastructure of the Human Stria Vascularis. PART I. *Acta Otolaryngol. (Stockh.)* 69, 415–427 (1970).
33. Jahnke, K. The fine structure of freeze-fractured intercellular junctions in the guinea pig inner ear. *Acta Oto-Laryngol. Suppl.* 336, 1–40 (1975).
34. Kitajiri, S. *et al.* Compartmentalization established by claudin-11-based tight junctions in stria vascularis is required for hearing through generation of endocochlear potential. *J. Cell Sci.* 117, 5087–5096 (2004).

35. Kharkovets, T. *et al.* Mice with altered KCNQ4 K+ channels implicate sensory outer hair cells in human progressive deafness. *EMBO J.* 25, 642–652 (2006).
36. Boettger, T. *et al.* Loss of K-Cl co-transporter KCC3 causes deafness, neurodegeneration and reduced seizure threshold. *EMBO J.* 22, 5422–5434 (2003).
37. Hama, K. & Saito, K. Gap junctions between the supporting cells in some acoustico-vestibular receptors. *J. Neurocytol.* 6, 1–12 (1977).
38. Minowa, O. *et al.* Altered cochlear fibrocytes in a mouse model of DFN3 nonsyndromic deafness. *Science* 285, 1408–1411 (1999).
39. Salt, A. N., Melichar, I. & Thalmann, R. Mechanisms of endocochlear potential generation by stria vascularis. *The Laryngoscope* 97, 984–991 (1987).
40. De Bold, A. J. Atrial natriuretic factor: a hormone produced by the heart. *Science* 230, 767–770 (1985).
41. Furuta, H., Mori, N., Luo, L. & Ryan, A. F. Detection of mRNA encoding guanylate cyclase A/atrial natriuretic peptide receptor in the rat cochlea by competitive polymerase chain reaction and in situ hybridization. *Hear. Res.* 92, 78–84 (1995).
42. Meyer zum Gottesberge, A. & Lamprecht, J. Localization of the atrial natriuretic peptide binding sites in the inner ear tissue--possibly an additional regulating system. *Acta Oto-Laryngol. Suppl.* 468, 53–57 (1989).
43. Piggott, L. A. *et al.* Natriuretic Peptides and Nitric Oxide Stimulate cGMP Synthesis in Different Cellular Compartments. *J. Gen. Physiol.* 128, 3–14 (2006).
44. Bryan, P. M. & Potter, L. R. The Atrial Natriuretic Peptide Receptor (NPR-A/GC-A) Is Dephosphorylated by Distinct Microcystin-sensitive and Magnesium-dependent Protein Phosphatases. *J. Biol. Chem.* 277, 16041–16047 (2002).
45. Potter, L. R. & Garbers, D. L. Protein kinase C-dependent desensitization of the atrial natriuretic peptide receptor is mediated by dephosphorylation. *J. Biol. Chem.* 269, 14636–14642 (1994).
46. Zografos, T. A. & Katritsis, D. G. Natriuretic Peptides as Predictors of Atrial Fibrillation Recurrences Following Electrical Cardioversion. 2, 109–14 (2013).
47. Shi, S.-J. *et al.* Natriuretic peptide receptor A mediates renal sodium excretory responses to blood volume expansion. *Am. J. Physiol. - Ren. Physiol.* 285, F694–F702 (2003).
48. Wall, S. M. & Weinstein, A. M. Cortical distal nephron Cl− transport in volume homeostasis and blood pressure regulation. *Am. J. Physiol. - Ren. Physiol.* 305, F427–F438 (2013).
49. Clarke, A. B., Trachte, G. J. & Fitzakerley, J. L. Inhibition of atrial natriuretic peptide degredation improves hearing. *SfN 42nd Annual Meeting* (2012).
50. Fitzakerley, J. L. & Trachte, G. J. The influence of natriuretic peptide A receptor knockout on hearing. *SfN 36th Annual Meeting* (2006).
51. Meyer zum Gottesberge, A. M., Gagelmann, M. & Forssmann, W. G. Atrial natriuretic peptide-like immunoreactive cells in the guinea pig inner ear. *Hear. Res.* 56, 86–92 (1991).
52. Long, L., Tang, Y., Xia, Q., Xia, Z. & Liu, J. The expression of atrial natriuretic peptide receptor in the mouse inner ear labyrinth. *Neuro Endocrinol. Lett.* 31, 126–130 (2010).

53. Qiao, L., Han, Y., Zhang, P., Cao, Z. & Qiu, J. Detection of atrial natriuretic peptide and its receptor in marginal cells and cochlea tissues from the developing rats. *Neuro Endocrinol. Lett.* 32, 187–192 (2011).
54. Furuta, H., Luo, L., Ryan, A. F. & Mori, N. Expression of mRNA encoding vasopressin V1a, vasopressin V2, and ANP-B receptors in the rat cochlea. *Hear. Res.* 117, 140–148 (1998).
55. Willott, J. F., Erway, L. C., Archer, J. R. & Harrison, D. E. Genetics of age-related hearing loss in mice. II. Strain differences and effects of caloric restriction on cochlear pathology and evoked response thresholds. *Hear. Res.* 88, 143–155 (1995).
56. Fan, D., Bryan, P. M., Antos, L. K., Potthast, R. J. & Potter, L. R. Down-Regulation Does Not Mediate Natriuretic Peptide-Dependent Desensitization of Natriuretic Peptide Receptor (NPR)-A or NPR-B: Guanylyl Cyclase-Linked Natriuretic Peptide Receptors Do Not Internalize. *Mol. Pharmacol.* 67, 174–183 (2005).
57. Nagase, M., Katafuchi, T., Hirose, S. & Fujita, T. Tissue distribution and localization of natriuretic peptide receptor subtypes in stroke-prone spontaneously hypertensive rats. *J. Hypertens.* 15, 1235–1243 (1997).
58. Lowe, D. G. *et al.* Human atrial natriuretic peptide receptor defines a new paradigm for second messenger signal transduction. *EMBO J.* 8, 1377–1384 (1989).
59. Schulz, S. *et al.* The primary structure of a plasma membrane guanylate cyclase demonstrates diversity within this new receptor family. *Cell* 58, 1155–1162 (1989).
60. Haas, M. & Forbush, B., 3rd. The Na-K-Cl cotransporter of secretory epithelia. *Annu. Rev. Physiol.* 62, 515–534 (2000).
61. Zeuthen, T. & Macaulay, N. Cotransport of water by Na^+-K^+-$2Cl^-$ cotransporters expressed in Xenopus oocytes: NKCC1 versus NKCC2. *J. Physiol.* 590, 1139–1154 (2012).
62. Park, J.-J. & Cunningham, M. G. Thin Sectioning of Slice Preparations for Immunohistochemistry. *J. Vis. Exp. JoVE* (2007). doi:10.3791/194
63. Kawaguchi, S. *et al.* Immunohistochemical localization of atrial natriuretic peptide receptor in bovine kidney and lung. *J. Histochem. Cytochem.* 37, 1739–1742 (1989).
64. Klokkers, J. *et al.* Atrial natriuretic peptide and nitric oxide signaling antagonizes vasopressin-mediated water permeability in inner medullary collecting duct cells. *Am. J. Physiol. - Ren. Physiol.* 297, F693–F703 (2009).
65. Hirsch, J. R. *et al.* Cellular localization, membrane distribution, and possible function of guanylyl cyclases A and 1 in collecting ducts of rat. *Cardiovasc. Res.* 51, 553–561 (2001).
66. Pandey, K. N. Guanylyl Cyclase/Atrial Natriuretic Peptide Receptor-A: Role in the Pathophysiology of Cardiovascular Regulation. *Can. J. Physiol. Pharmacol.* 89, 557–573 (2011).
67. Ginns, S. M. *et al.* Immunolocalization of the secretory isoform of Na-K-Cl cotransporter in rat renal intercalated cells. *J. Am. Soc. Nephrol. JASN* 7, 2533–2542 (1996).
68. Hibino, H. *et al.* Expression of an inwardly rectifying K+ channel, Kir5.1, in specific types of fibrocytes in the cochlear lateral wall suggests its functional importance in the establishment of endocochlear potential. *Eur. J. Neurosci.* 19, 76–84 (2004).

69. Liu, C. *et al.* Inhibition of dehydration-induced water intake by glucocorticoids is associated with activation of hypothalamic natriuretic peptide receptor-A in rat. *PloS One* 5, e15607 (2010).
70. Abbey, S. E. & Potter, L. R. Vasopressin-dependent Inhibition of the C-type Natriuretic Peptide Receptor, NPR-B/GC-B, Requires Elevated Intracellular Calcium Concentrations. *J. Biol. Chem.* 277, 42423–42430 (2002).
71. Jenkins, N. T., Padilla, J., Rector, R. S. & Laughlin, M. H. Influence of regular physical activity and caloric restriction on β-adrenergic and natriuretic peptide receptor expression in retroperitoneal adipose tissue of OLETF rats. *Exp. Physiol.* 98, 1576–1584 (2013).
72. Vilotti, S., Marchenkova, A., Ntamati, N. & Nistri, A. B-Type Natriuretic Peptide-Induced Delayed Modulation of TRPV1 and P2X3 Receptors of Mouse Trigeminal Sensory Neurons. *PLoS ONE* 8, (2013).
73. Lu, H.-L. *et al.* Gastric nNOS reduction accompanied by natriuretic peptides signaling pathway upregulation in diabetic mice. *World J. Gastroenterol. WJG* 20, 4626–4635 (2014).
74. Liu, X.-Y. *et al.* B-type natriuretic peptide is neither itch-specific nor functions upstream of the GRP-GRPR signaling pathway. *Mol. Pain* 10, 4 (2014).
75. Stanbury, J. B., Kassenaar, A. A. H., Meijer, J. W. A. & Terpstra, J. The metabolism of iodotyrosines. I. The fate of mono- and di-iodotyrosine in normal subjects and in patients with various diseases. *J. Clin. Endocrinol. Metab.* 16, 735–746 (1956).
76. Friedman, J. E., Watson, J. A., Lam, D. W.-H. & Rokita, S. E. Iodotyrosine Deiodinase Is the First Mammalian Member of the NADH Oxidase/Flavin Reductase Superfamily. *J. Biol. Chem.* 281, 2812–2819 (2006).
77. Chan, C.-B. *et al.* Mice lacking asparaginyl endopeptidase develop disorders resembling hemophagocytic syndrome. *Proc. Natl. Acad. Sci.* 106, 468–473 (2009).
78. Zhao, L. *et al.* Structural analysis of asparaginyl endopeptidase reveals the activation mechanism and a reversible intermediate maturation stage. *Cell Res.* 24, 344–358 (2014).
79. Potter, L. R. Guanylyl cyclase structure, function and regulation. *Cell. Signal.* 23, 1921–1926 (2011).
80. Lowe, D. G. & Fendly, B. M. Human natriuretic peptide receptor-A guanylyl cyclase. Hormone cross-linking and antibody reactivity distinguish receptor glycoforms. *J. Biol. Chem.* 267, 21691–21697 (1992).
81. Killick, R. & Richardson, G. P. Antibodies to the sulphated, high molecular mass mouse tectorin stain hair bundles and the olfactory mucus layer. *Hear. Res.* 103, 131–141 (1997).
82. Legan, P. K. *et al.* A Targeted Deletion in α-Tectorin Reveals that the Tectorial Membrane Is Required for the Gain and Timing of Cochlear Feedback. *Neuron* 28, 273–285 (2000).
83. Bonhomme, M. C. *et al.* Immunolocalization of natriuretic peptide receptor B in the rat kidney. *J. Am. Soc. Nephrol.* 9, 1777–1786 (1998).

84. Ritter, D., Dean, A. D., Gluck, S. L. & Greenwald, J. E. Natriuretic peptide receptors A and B have different cellular distributions in rat kidney. *Kidney Int.* 48, 5758–5766 (1995).
85. Kaplan, M. R., Plotkin, M. D., Brown, D., Hebert, S. C. & Delpire, E. Expression of the mouse Na-K-2Cl cotransporter, mBSC2, in the terminal inner medullary collecting duct, the glomerular and extraglomerular mesangium, and the glomerular afferent arteriole. *J. Clin. Invest.* 98, 723–730 (1996).
86. Cao, L.-H. & Yang, X.-L. Natriuretic peptides and their receptors in the central nervous system. *Prog. Neurobiol.* 84, 234–248 (2008).
87. Kawano, H. & Masuko, S. Region-specific projections from the subfornical organ to the paraventricular hypothalamic nucleus in the rat. *Neuroscience* 169, 1227–1234 (2010).
88. Smith, P. M. & Ferguson, A. V. Cardiovascular actions of leptin in the subfornical organ are abolished by diet-induced obesity. *J. Neuroendocrinol.* 24, 504–510 (2012).
89. Andres, K. H., von Düring, M. & Veh, R. W. Subnuclear organization of the rat habenular complexes. *J. Comp. Neurol.* 407, 130–150 (1999).
90. Kharkovets, T. *et al.* KCNQ4, a K+ channel mutated in a form of dominant deafness, is expressed in the inner ear and the central auditory pathway. *Proc. Natl. Acad. Sci. U. S. A.* 97, 4333–4338 (2000).
91. Hama, K. & Saito, K. Gap junctions between the supporting cells in some acoustico-vestibular receptors. *J. Neurocytol.* 6, 1–12 (1977).
92. Paulson, A. F. *et al.* Cyclic AMP and LDL trigger a rapid enhancement in gap junction assembly through a stimulation of connexin trafficking. *J. Cell Sci.* 113 (Pt 17), 3037–3049 (2000).
93. Oyamada, M., Oyamada, Y. & Takamatsu, T. Regulation of connexin expression. *Biochim. Biophys. Acta BBA - Biomembr.* 1719, 6–23 (2005).
94. Kanaporis, G. *et al.* Gap junction channels exhibit connexin-specific permeability to cyclic nucleotides. *J. Gen. Physiol.* 131, 293–305 (2008).
95. Kikuchi, T., Kimura, R. S., Paul, D. L., Takasaka, T. & Adams, J. C. Gap junction systems in the mammalian cochlea. *Brain Res. Brain Res. Rev.* 32, 163–166 (2000).
96. Trowe, M.-O. *et al.* Impaired stria vascularis integrity upon loss of E-cadherin in basal cells. *Dev. Biol.* 359, 95–107 (2011).
97. Abraham, R. L., Yang, T., Blair, M., Roden, D. M. & Darbar, D. Augmented potassium current is a shared phenotype for two genetic defects associated with familial atrial fibrillation. *J. Mol. Cell. Cardiol.* 48, 181–190 (2010).
98. Ritchie, M. D. *et al.* Chromosome 4q25 Variants Are Genetic Modifiers of Rare Ion Channel Mutations Associated With Familial Atrial Fibrillation. *J. Am. Coll. Cardiol.* 60, 1173–1181 (2012).
99. Lamprecht, J. & Meyer zum Gottesberge, A. M. The presence and localization of receptors for atrial natriuretic peptide in the inner ear of the guinea pig. *Arch. Otorhinolaryngol.* 245, 300–301 (1988).

100. Guipponi, M. *et al.* An integrated genetic and functional analysis of the role of type II transmembrane serine proteases (TMPRSSs) in hearing loss. *Hum. Mutat.* 29, 130–141 (2008).
101. Pandey, K. N. Stimulation of protein phosphorylation by atrial natriuretic factor in plasma membranes of bovine adrenal cortical cells. *Biochem. Biophys. Res. Commun.* 163, 988–994 (1989).
102. Trachte, G. J. & Fitzakerley, J. L. in *Natriuret. Pept. Physiol. Mol. Biol. Clin. Implic.* (ed. Pandey, K. N.) 237–258 (Nova Science Publishers Inc., 2014).
103. Bryan, P. M. *et al.* A sensitive method for determining the phosphorylation status of natriuretic peptide receptors: cGK-Ialpha does not regulate NPR-A. *Biochemistry (Mosc.)* 45, 1295–1303 (2006).
104. Sunose, H., Ikeda, K., Suzuki, M. & Takasaka, T. Voltage-activated K channel in luminal membrane of marginal cells of stria vascularis dissected from guinea pig. *Hear. Res.* 80, 86–92 (1994).
105. Marcus, D. C. & Shen, Z. Slowly activating voltage-dependent K+ conductance is apical pathway for K+ secretion in vestibular dark cells. *Am. J. Physiol.* 267, C857–864 (1994).
106. Zhang, J. *et al.* Atrial natriuretic peptide modulates the proliferation of human gastric cancer cells via KCNQ1 expression. *Oncol. Lett.* 6, 407–414 (2013).
107. Denoyelle, F. *et al.* Connexin 26 gene linked to a dominant deafness. *Nature* 393, 319–320 (1998).
108. Eckhard, A. *et al.* Water channel proteins in the inner ear and their link to hearing impairment and deafness. *Mol. Aspects Med.* 33, 612–637 (2012).
109. Lopez, I. A., Ishiyama, G., Lee, M., Baloh, R. W. & Ishiyama, A. Immunohistochemical localization of aquaporins in the human inner ear. *Cell Tissue Res.* 328, 453–460 (2007).
110. Taguchi, D. *et al.* Expression and immunolocalization of aquaporin-6 (Aqp6) in the rat inner ear. *Acta Otolaryngol. (Stockh.)* 128, 832–840 (2008).